Supporting Information

Rapid and Profound Rewiring of Brain Lipid Signaling Networks by Acute Diacylglycerol Lipase Inhibition

Daisuke Ogasawara, Hui Deng, Andreu Viader, Marc P. Baggelaar, Arjen C. Breman, Hans den Dulk, Adriaan M.C.H. van den Nieuwendijk, Marjolein Soethoudt,Tom van der Wel, Juan Zhou, Hermen S. Overkleeft, Manuel Sanchez-Alavez, Simone Mori, William Nguyen, Bruno Conti, Xiaojie Liu, Yao Chen, Qing-song Liu, Benjamin F. Cravatt, Mario van der Stelt

Supporting Figures, Tables, and Data sets

Table S1. Inhibitory values for DH376, DO34, and DO53 versus recombinant and native DAGL enzymes using the indicated assays. Data represent average values ± SD; n = 4 per group.

		pIC_{50}	
Enzyme	Compound	DAGLα	DAGLβ
Recombinant enzymes (SAG hydrolysis assay)			
	DH376	8.2 ± 0.3	8.6 ± 0.3
	DO34	8.2 ± 0.3	8.1 ± 0.3
	DO53	5.6 ± 0.4	7.0 ± 0.2
Brain enzymes ABPP (DH379)			
	DH376	9.2 ± 0.1	8.6 ± 0.1
	DO34	9.1 ± 0.1	8.6 ± 0.1
	DO53	7.4 ± 0.1	7.6 ± 0.1
Brain enzymes ABPP (HT-01)			
	DH376	8.9 ± 0.1	8.3 ± 0.1
	DO34	9.3 ± 0.1	8.6 ± 0.1
	DO53	7.6 ± 0.1	7.1 ± 0.1

Dataset S1. Complete proteomic data for ABPP-reductive demethylation analysis of brain serine hydrolase activities from mice treated with DH376, DO34 and DO53 (50 mg/kg, i.p., 4 h treatment).

See accompanying excel file.

Dataset S2. Brain lipid profiles for DAGL inhibitor-treated or DAGL$\alpha^{-/-}$ mice. Data represent average values ± s.e.m.; n = 5-6 per group. Data were analyzed statistically by the student's t test (unpaired, two-tailed) for inhibitor-treated or DAGL$\alpha^{-/-}$ groups versus vehicle control group and subject to a Benjamini Hochberg correction where the false discovery rate was set to 10%. Post-correction p values < 0.007 were designated as significant and are marked in red. We have also listed p values between 0.007 and 0.05 in blue, with remaining p values designated as NS (not significant).

See accompanying excel file.

Supporting Figures

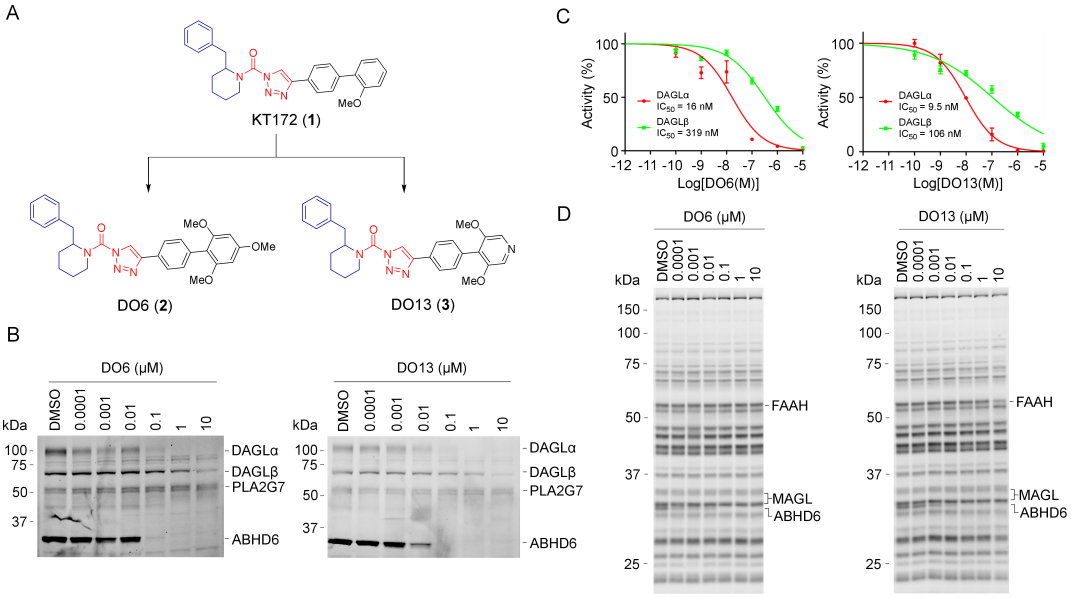

Fig. S1. Analogs of KT172 with leaving group modifications that improve DAGLα inhibitory activity. (**A**) Chemical structures of original DAGL inhibitor KT172 and analogs DO6 and DO13 bearing modifications to the distal phenyl ring appended to the triazole leaving group. (**B**) Concentration-dependent inhibition of DAGLα and DAGLβ activity by DO6 and DO13 as measured by competitive ABPP of mouse brain proteome using the HT-01 probe (1 μM, 30 min). Additional serine hydrolases detected by HT-01 are labeled. (**C**) Quantification of data shown in (**B**). Data represent average values ± SD; n = 3 per group. (**D**) Selectivity profiles of DH376, DO34, and DO53 across mouse brain serine hydrolases as determined by competitive ABPP using the FP-Rh probe (1 μM, 30 min). Representative mouse brain serine hydrolases detected by FP-Rh are labeled.

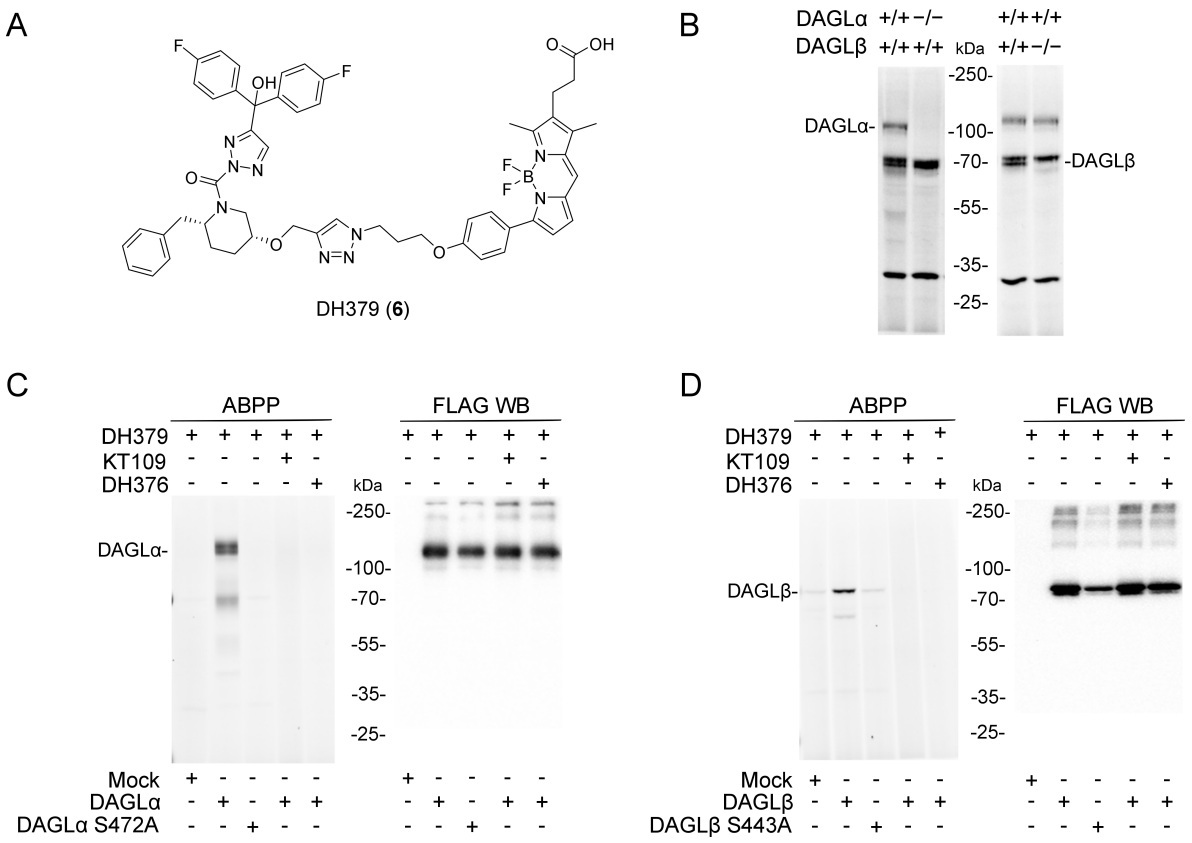

Fig. S2. Characterization of a DH379, a DAGL-tailored activity-based probe. (**A**) Chemical structure of DH379. (**B**) Labeling and detection of endogenous DAGLα and DAGLβ in mouse brain membrane proteome by DH379 (1 μM, 20 min). The assignment of DH379-labeled proteins as DAGLα and DAGLβ was confirmed by analyzing brain membrane proteomes from wild type and DAGLα$^{-/-}$ and DAGLβ$^{-/-}$ mice. (**C, D**) Left panels, DH379 labels recombinant, FLAG epitope-tagged wild type DAGLα (**C**) and DAGLβ (**D**), but not their catalytically inactive serine mutants (S472A and S443A, respectively) or DAGL enzymes that have been pre-treated with inhibitors KT109 or DH376 (1 μM, 30 min). Right panels, western blots showing DAGL enzyme expression level in transfected HEK293T cells as determined with an anti-FLAG antibody.

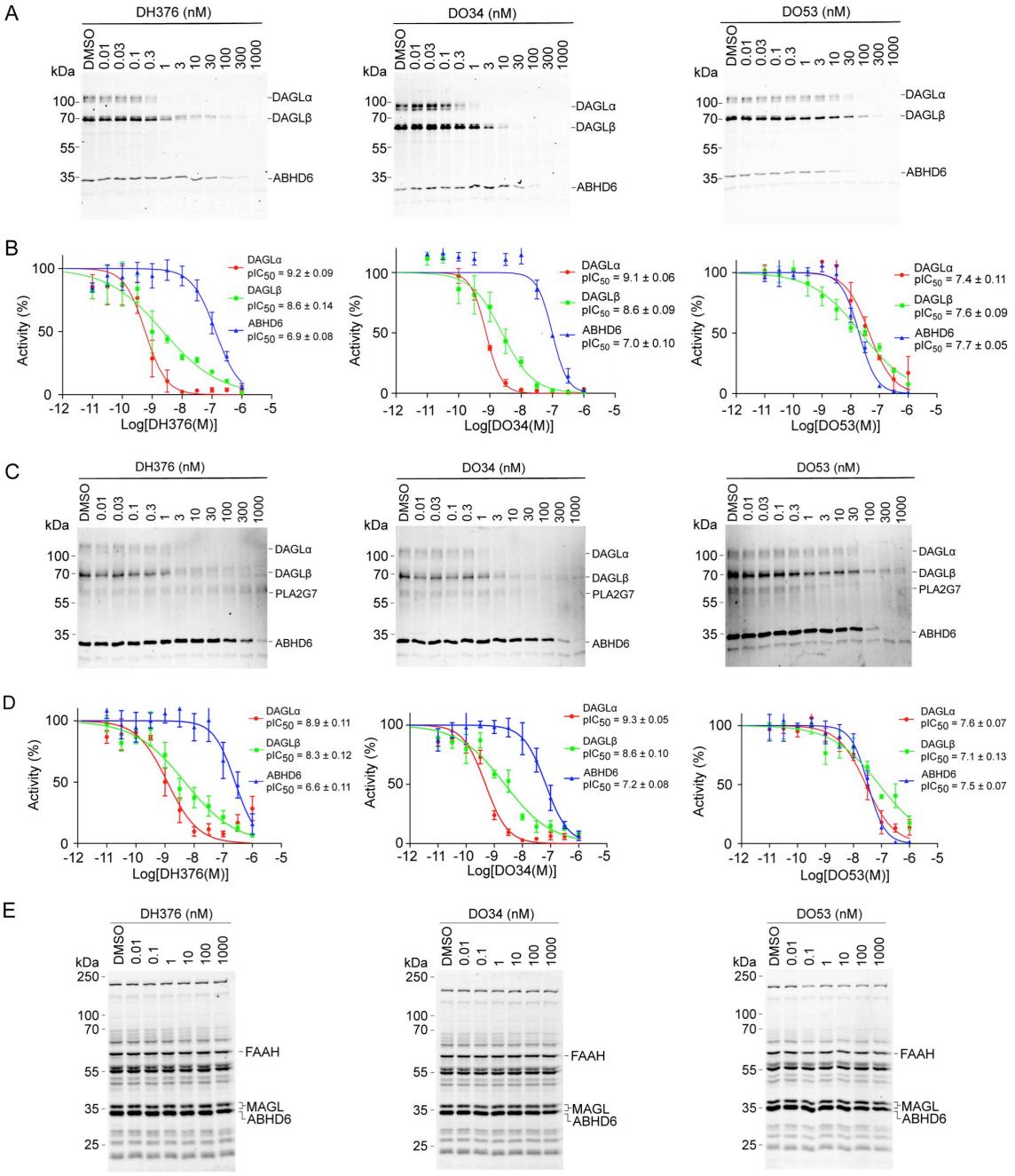

Fig. S3. Additional *in vitro* characterization of DAGL inhibitors. (**A**) Concentration-dependent inhibition of DAGLα and DAGLβ activity by DH376, DO34 and DO53 as measured by gel-based competitive ABPP of mouse brain proteome using the tailored

activity-based probe DH379 (1 μM, 30 min). (**B**) Quantification of data shown in (**A**). Data represent average values ± SEM; n = 3 per group. (**C**) Concentration-dependent inhibition of DAGLα, DAGLβ, and ABHD6 by DH376, DO34 and DO53 as measured by gel-based competitive ABPP of mouse brain proteome using the HT-01 probe (1 μM, 30 min). (**D**) Quantification of data shown in (**C**). Data represent average values ± SEM; n = 3 per group. (**E**) Selectivity profiles of DH376, DO34, and DO53 across mouse brain serine hydrolases as determined by competitive ABPP using the broad-spectrum probe FP-Rh (0.5 μM, 20 min). Representative mouse brain serine hydrolases detected by FP-Rh are labeled. Note that, in these gel profiles for FP-Rh labeling, the ABHD6 and MAGL signals were not resolved from one another (and DAGLα and DAGLβ are not visualized due to overlapping migration patterns with more abundant serine hydrolases).

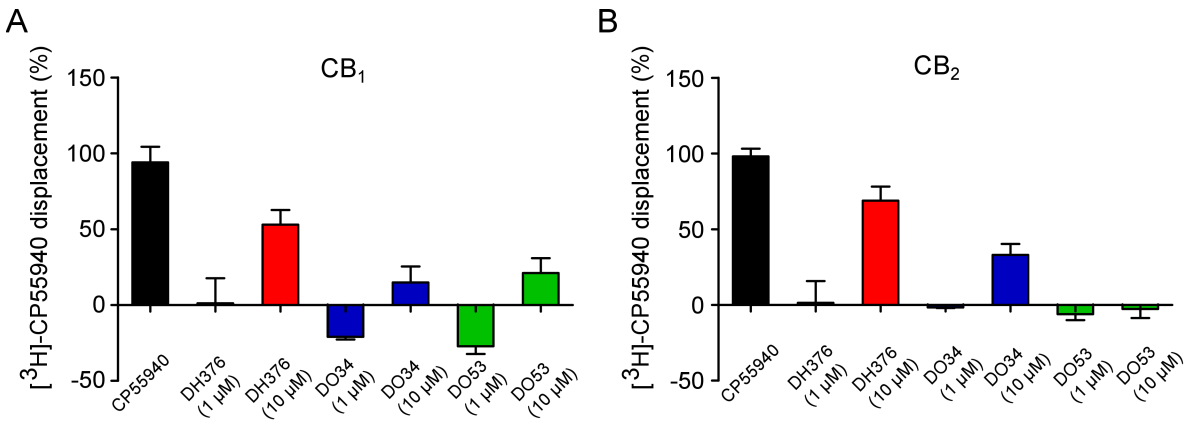

Fig. S4. DH376 and DO34 show minimal interactions with cannabinoid receptors CB_1R and CB_2R. DH376 and DO34 were tested for binding affinity to the CB1R and CB2R using competition studies with the radiolabeled CBR ligand [^{3}H]-CP55940 using membranes from recombinant human CB1R- and CB2R-overexpressing CHO cells. DO34 was inactive at 10 μM and DH376 was inactive at 1 μM and showed only partial (~50% for CB1, ~70% for CB2) inhibition of ligand binding at 10 μM.

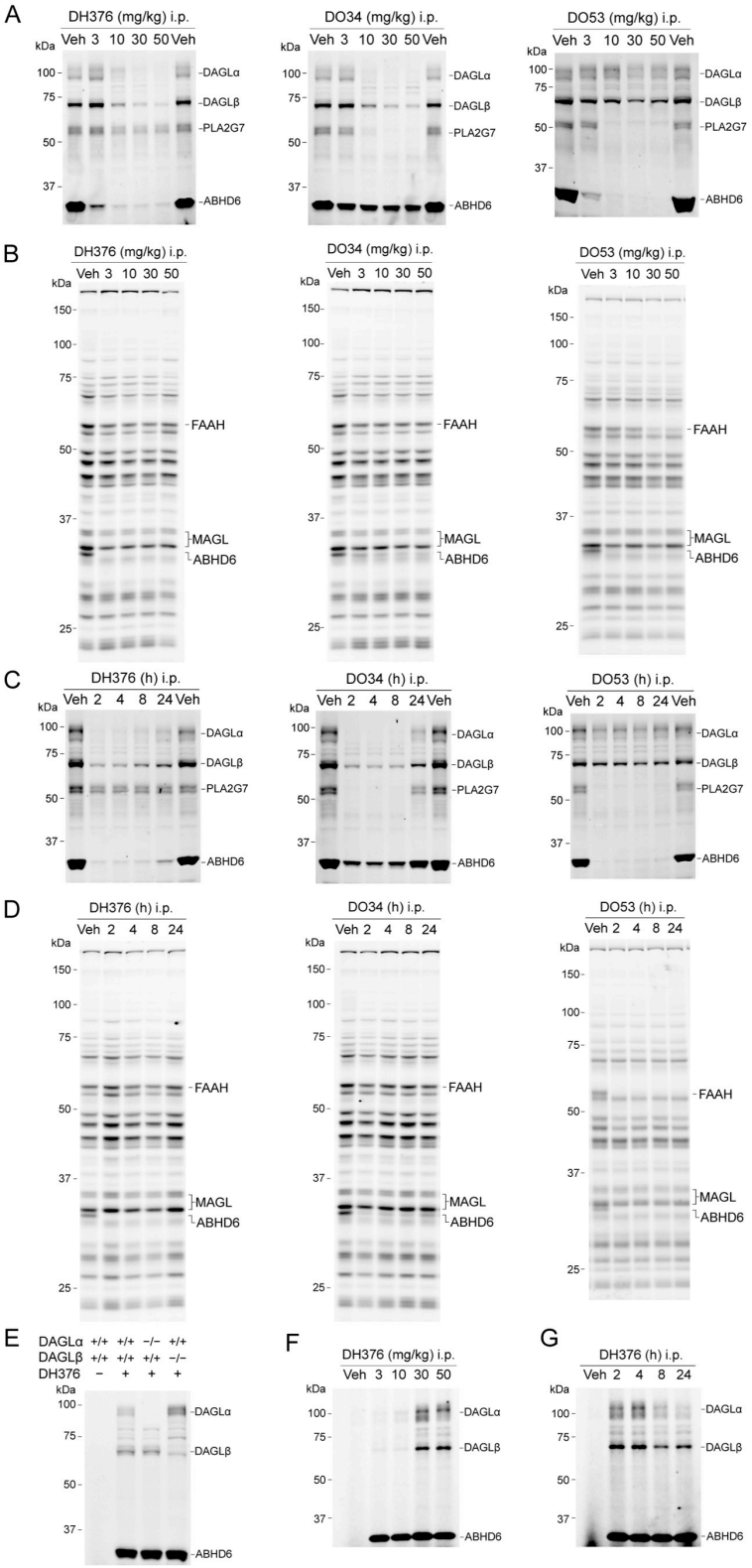
A
DH376 (mg/kg) i.p.
Veh 3 10 30 50 Veh
DO34 (mg/kg) i.p.
Veh 3 10 30 50 Veh
DO53 (mg/kg) i.p.
Veh 3 10 30 50 Veh
kDa
100
75
50
37
DAGLα
DAGLβ
PLA2G7
ABHD6
B
DH376 (mg/kg) i.p.
Veh 3 10 30 50
DO34 (mg/kg) i.p.
Veh 3 10 30 50
DO53 (mg/kg) i.p.
Veh 3 10 30 50
kDa
150
100
75
50
37
25
FAAH
MAGL
ABHD6
C
DH376 (h) i.p.
Veh 2 4 8 24 Veh
DO34 (h) i.p.
Veh 2 4 8 24 Veh
DO53 (h) i.p.
Veh 2 4 8 24 Veh
kDa
100
75
50
37
DAGLα
DAGLβ
PLA2G7
ABHD6
D
DH376 (h) i.p.
Veh 2 4 8 24
DO34 (h) i.p.
Veh 2 4 8 24
DO53 (h) i.p.
Veh 2 4 8 24
kDa
150
100
75
50
37
25
FAAH
MAGL
ABHD6
E
DAGLα +/+ +/+ −/− +/+
DAGLβ +/+ +/+ +/+ −/−
DH376 − + + +
kDa
100
75
50
37
DAGLα
DAGLβ
ABHD6
F
DH376 (mg/kg) i.p.
Veh 3 10 30 50
kDa
100
75
50
37
DAGLα
DAGLβ
ABHD6
G
DH376 (h) i.p.
Veh 2 4 8 24
kDa
100
75
50
37
DAGLα
DAGLβ
ABHD6

Fig. S5. Further studies assessing the *in vivo* activity and selectivity of DH376, DO34, and DO53 in mice. (**A**, **B**) Assessment of dose-dependent inhibition of DAGLα and DAGLβ and cross-reactivity with other serine hydrolases in brain tissue from mice treated with vehicle (Veh) or DO34, DH376, or DO53 (i.p., 4 h) as determined by competitive ABPP using the HT-01 (**A**) or FP-Rh (**B**) probe (1 μM, 30 min). (**C**, **D**) Assessment of time course of inhibition of DAGLα and DAGLβ and cross-reactivity with other serine hydrolases in brain tissue from mice treated with vehicle or DO34, DO376, or DO53 (50 mg/kg, i.p.) as determined by competitive ABPP using the HT-01 (**C**) or FP-Rh (**D**) probe (1 μM, 30 min). (**E**) Confirmation of direct, *in vivo*-labeling of DAGLα and DAGLβ by DH376 (50 mg/kg, i.p., 4 h) visualized by CuAAC to a Cy5 reporter group. The assignment of DH376-labeled proteins as DAGLα and DAGLβ was confirmed by analyzing brain membrane proteomes from wild type and DAGLα$^{-/-}$ and DAGLβ$^{-/-}$ mice. (**F, G**) Dose-dependency (**F**) and time course (**G**) of direct, *in vivo*-labeling of DAGLα and DAGLβ ABPP in brain tissue from mice treated with DH376 (i.p., 4 h for dose-dependency; 50 mg/kg, i.p. for time course) visualized by CuAAC to a Cy5 reporter group.

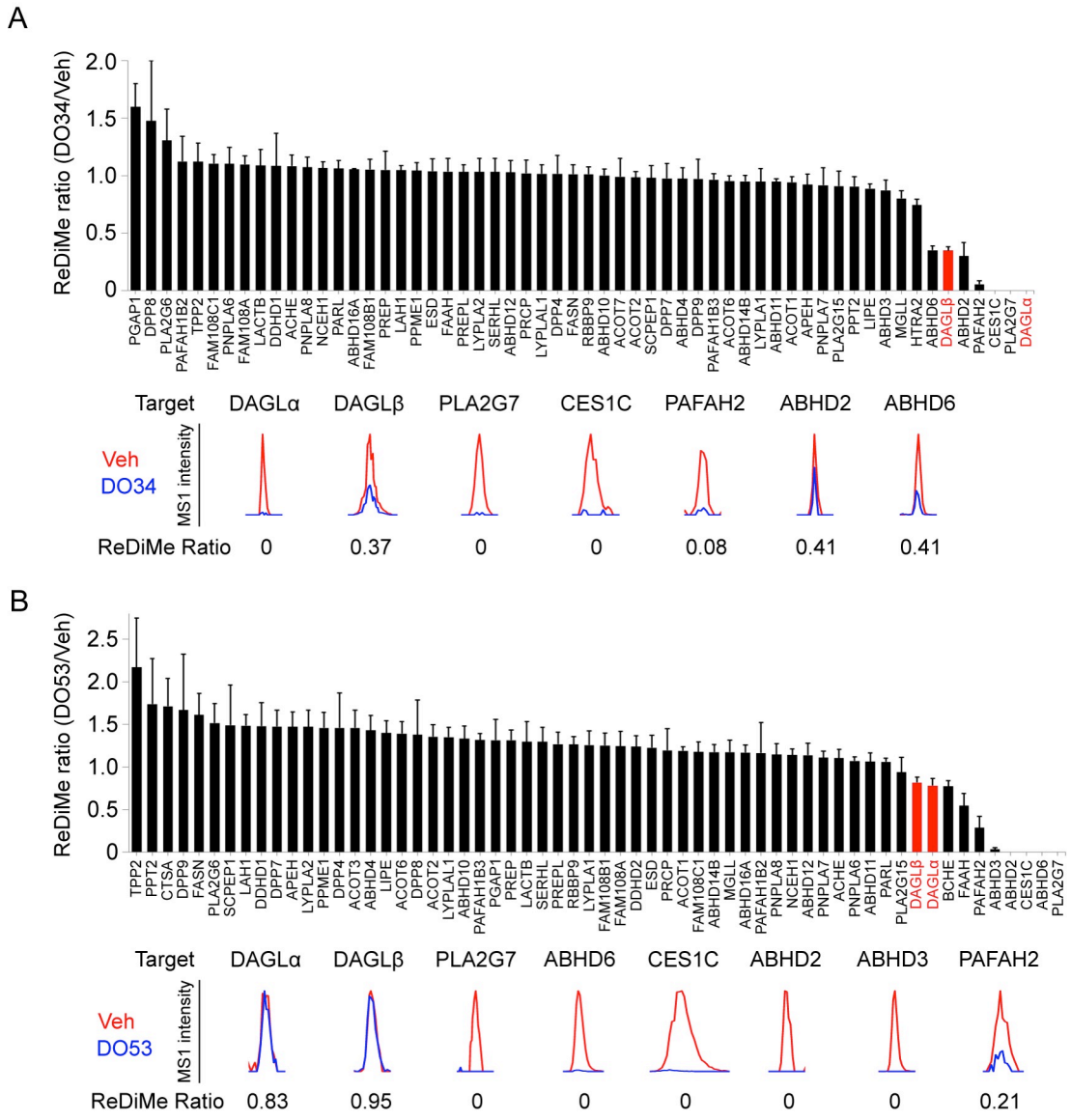

Fig. S6. Assessment of *In vivo* activity and selectivity of DO34 and DO53 by ABPP-ReDiMe analysis. ABPP-ReDiMe analysis of brain serine hydrolase activities from mice treated with DO34 (**A**) and DO53 (**B**) (50 mg/kg, i.p., 4 h treatment), where serine hydrolases were labeled and enriched using an FP-biotin probe (1). Representative MS1 chromatograms for DAGLα and DAGLβ, as well as additional serine hydrolase targets are shown for each inhibitor. Data represent average values ± SEM; n = 3−4 mice per group.

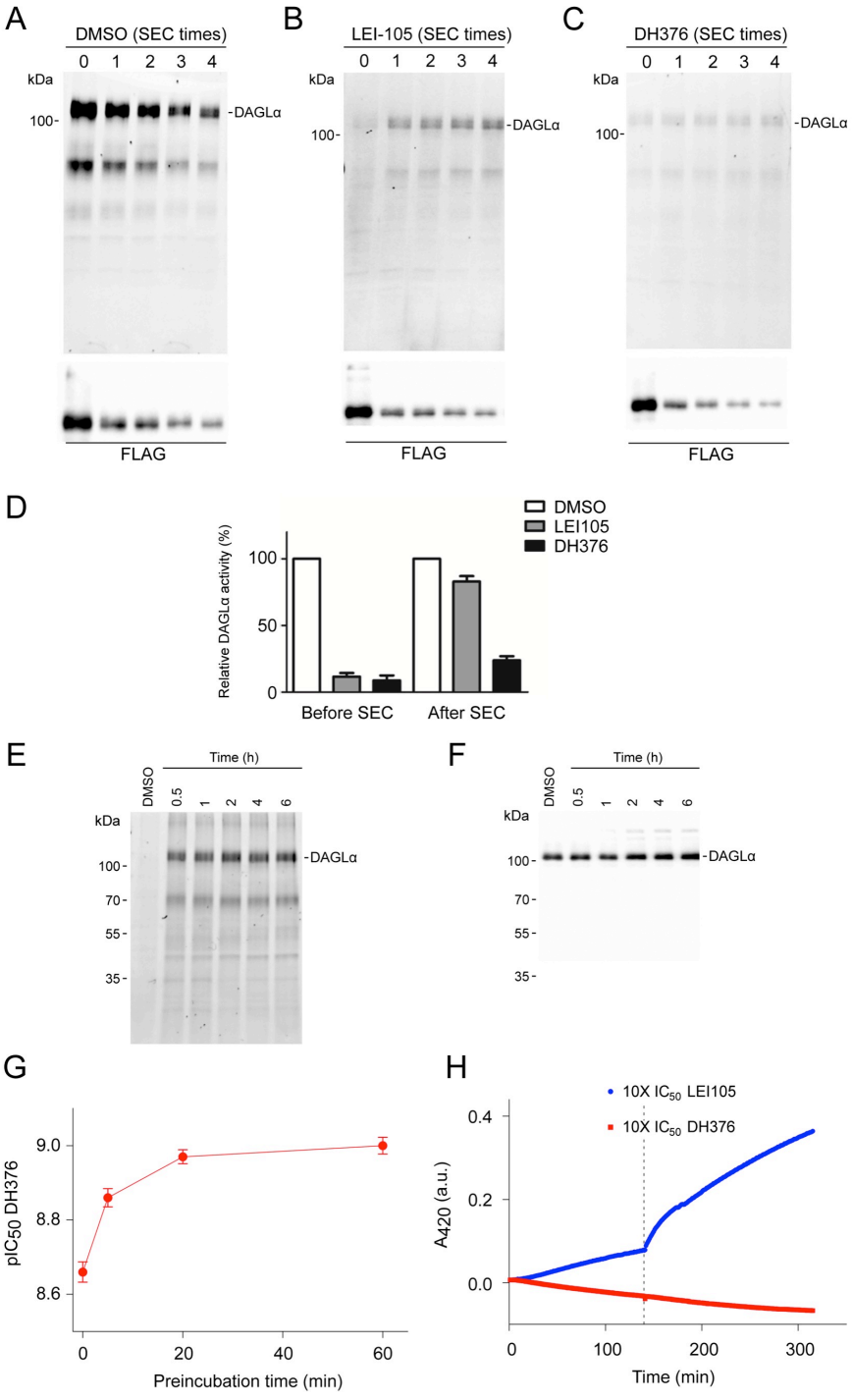

Fig. S7. Assessing the reversibility of DH376 reactivity with recombinant human DAGLα. (**A–C**) Recovery of DAGLα activity after exposing the indicated inhibitor (or

control)-treated samples to serial size exclusion chromatography (SEC) steps, where activity was measured by gel-based ABPP using the DH379 probe. Note that little or no DH379 labeling was observed post-SEC in DH376-treated DAGLα samples (**C**), while substantial DH379 labeling was observed post-SEC for DAGLα samples treated with the reversible inhibitor LEI105 (**B**). Western blots using anti-FLAG antibodies are shown to assess protein loading. (**D**) Quantification of the data shown in (**A−C**) after four SEC steps. Data represent average values ± SD; n = 3 per group. (**E**) Assessment of stability of the DH376-DAGLα adduct. Recombinant human DAGLα expressed in transfected HEK293T cell proteomes was treated with DH376 (10 nM) for 30 min and the reaction was exposed to five serial SEC steps and then incubated for the indicated times (0.5-6 h) before visualization by CuAAC to a Cy5 reporter group. No appreciable loss of signal intensity for the DH376-DAGLα adduct was observed across the time course analysis. (**F**) Western blot using anti-FLAG antibodies is shown to assess protein loading. (**G**) Plot of IC_{50} values for DH376 inhibition of DAGLα measured after the indicated pre-incubation times prior to analysis with a para-nitrophenylbutyrate (PNP) substrate (300 μM) (2). Data represent average values ± SD; n = 4 per group. (**H**) DAGLα product progression curves as a function of time in the presence of PNP substrate (300 μM) and 10X IC_{50} value concentrations of LEI105 or DH376. After 135 min, a second batch of PNP (300 μM) was added to the reaction vessel. Note that the enzymatic rate of PNP conversion is increased in the LEI105-treated sample (blue line), whereas no effect is observed in enzyme inhibited by DH376 (red line). Shown is a representative experiment of four replicate experiments.

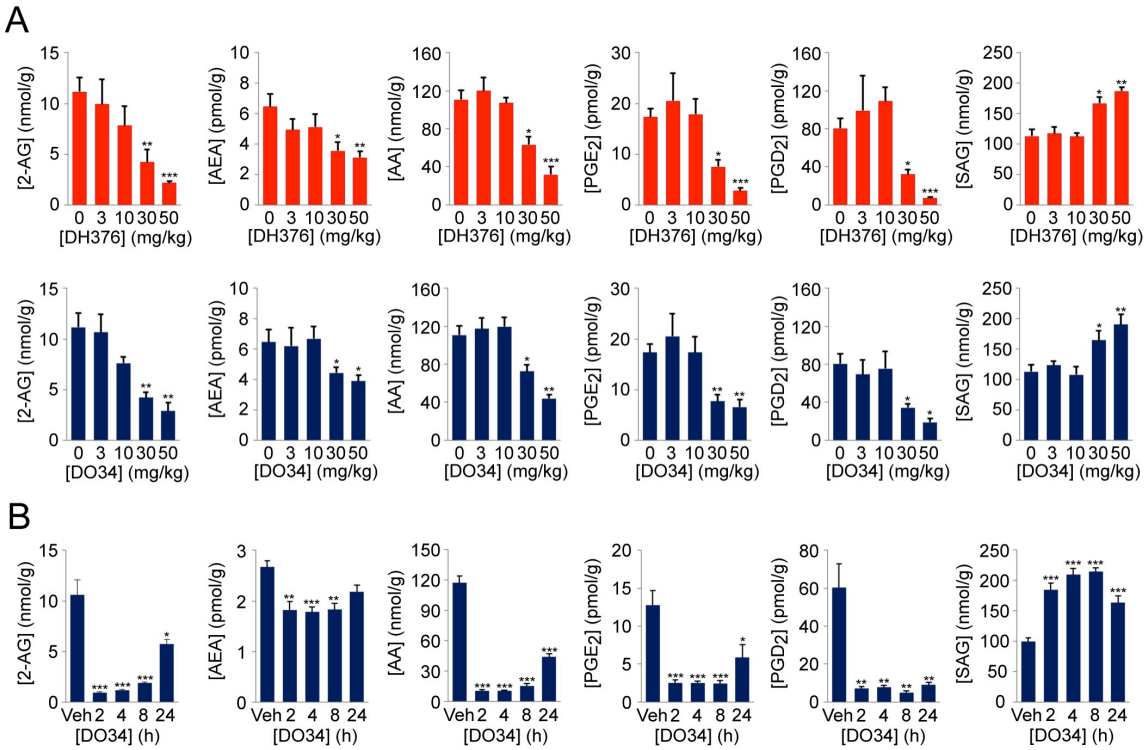

Fig. S8. Dose- and time-dependent changes in brain lipids in mice treated with DAGL inhibitors. (**A**) Dose-dependent changes in 2-AG and other bioactive lipids in brain tissue from mice treated with DH376 and DO34 (i.p., 4 h). Data represent average values ± SEM; n = 3−4 mice per group. *p < 0.05; **p < 0.01; ***p < 0.001 for inhibitor-treated vs vehicle-treated (0 mg/kg) mice. (**B**) Time-dependent changes in 2-AG and other bioactive lipids in brain tissue from mice treated with DO34 (50 mg/kg, i.p.). Data represent average values ± SEM; n = 3−4 mice per group. *p < 0.05; **p < 0.01; ***p < 0.001 for inhibitor-treated vs. vehicle-treated mice.

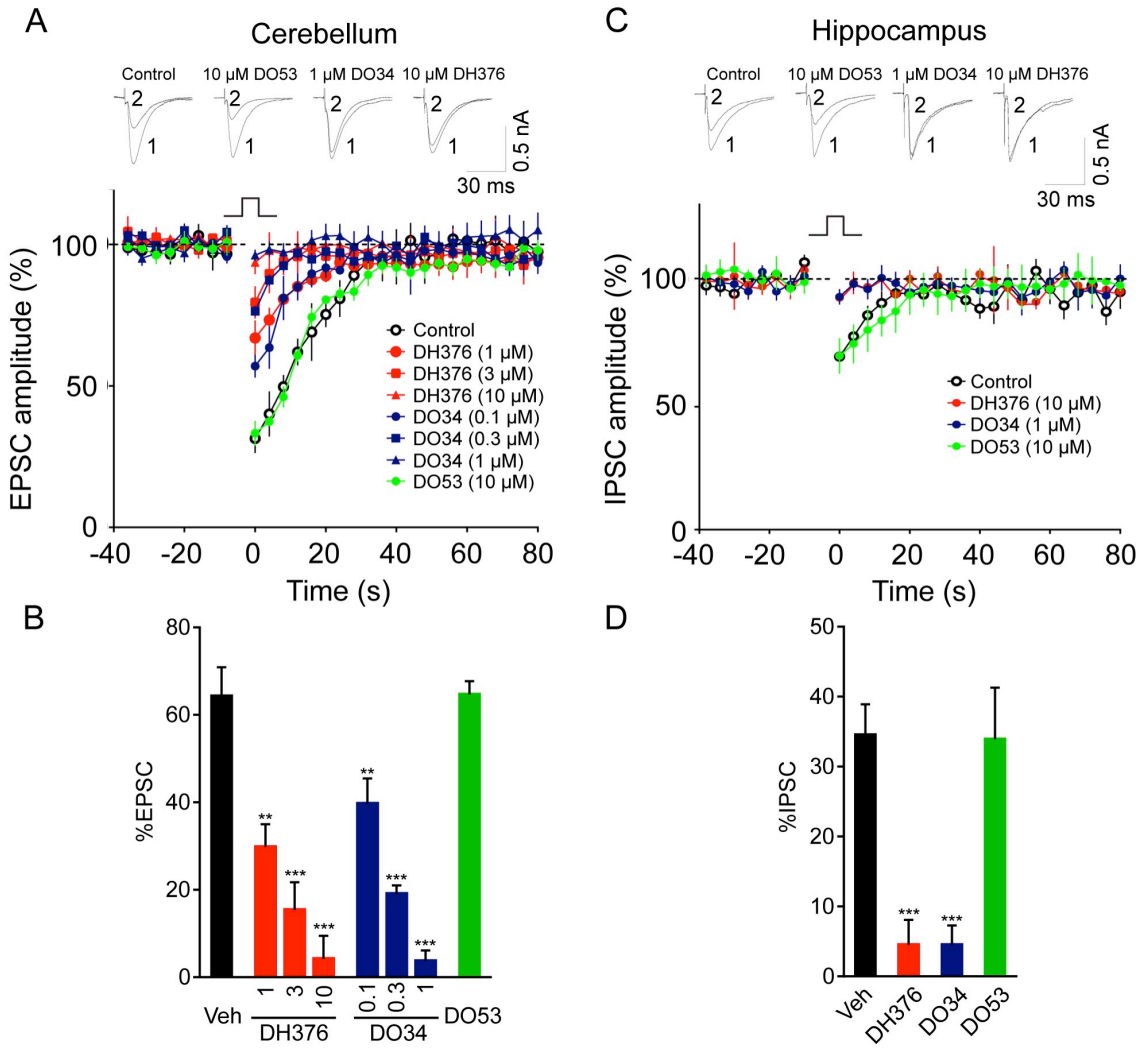

Fig. S9. Acute inhibition of DAGLs fully blocks endocannabinoid-mediated forms of synaptic plasticity. (**A**, **B**) Sample traces and average time course (**A**) and magnitude (**B**) of parallel fiber-excitatory postsynaptic currents (PF-EPSCs) in response to a brief depolarization in cerebellar slices following treatment (30 min) with vehicle, DH376 (1-10 μM), DO34 (0.1−1 μM), or DO53 (10 μM). Data represent average values ± SEM; n = 5-10 samples per group. (**C**, **D**) Sample traces and average time course (**C**) and magnitude (**D**) of inhibitory postsynaptic currents (IPSCs) in CA1 pyramidal neurons in response to a brief depolarization in hippocampal slices following treatment (30 min) with vehicle, DH376 (10

μM), DO34 (1 μM), and DO53 (10 μM). Data represent average values ± SEM; n = 7−8 samples per group. *$p < 0.05$; **$p < 0.01$; ***$p < 0.001$ vs. vehicle-treated samples.

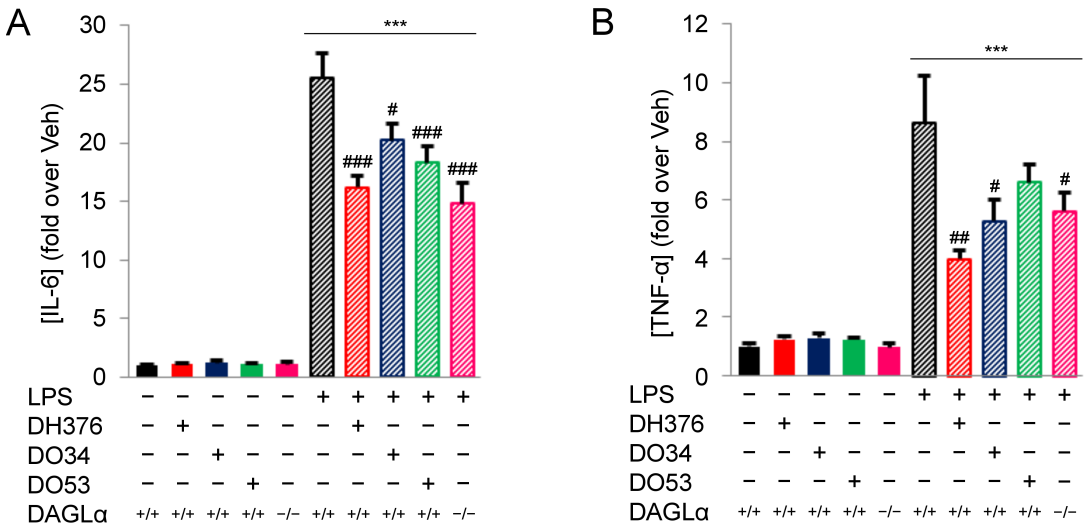

Fig. S10. Disruption of DAGLs reduces brain inflammatory cytokine production in LPS-treated mice. Quantification of IL-6 (**A**) and TNF-α (**B**) cytokines in brain tissue from mice treated with DH376-, DO34-, and DO53-treated (50 mg/kg, i.p., 1−1.5 h) or DAGLα$^{-/-}$ mice with or without subsequent treatment with LPS (20 mg/kg, i.p., 6 h). Data represent average values ± SEM; n = 5−8 mice per group. ***p < 0.001 for all groups vs. vehicle-treated DAGLα$^{+/+}$ mice; $^{\#}$p < 0.05; $^{\#\#}$p < 0.01; $^{\#\#\#}p$ < 0.001 for all groups vs. LPS-treated DAGLα$^{+/+}$ mice.

Supporting Experimental Procedures

Materials. Triazole urea compounds and LEI105 were synthesized in the laboratory following previously described procedures (3, 4). Fluorophosphonate (FP)-rhodamine, FP-biotin and HT-01 were synthesized according to a previously described protocol (1, 5-7). FP-rhodamine is also commercially available at Thermo Fischer Scientific. All deuterated lipid standards and substrates were purchased from Cayman Chemicals.

DAGLα/β plasmids. For the preparation of the different constructs, full length human cDNA was purchased from Source Bioscience and mouse cDNA was purchased from Open Biosystems, and were cloned into mammalian expression vector pcDNA3.1, containing genes for ampicillin and neomycin resistance. DAGLα/β constructs were obtained as reported previously (2, 8). For proteins containing a FLAG-tag, a FLAG-linker was made from primers and cloned into the vector at the C-terminus of hDAGLα or hDAGLβ. Two step PCR mutagenesis was performed to substitute the active site serine for an alanine in the hDAGLβ-FLAG, to obtain hDAGLβ-S443A-FLAG. Plasmids were isolated from transformed XL-10 Z-competent cells (Maxi Prep, Qiagen) and verified by Sanger sequencing (BaseClear).

Cell culture and membrane preparation. Cell culture and membrane preparation were performed as previously described (2). In brief, HEK293T cells were grown in DMEM with stable glutamine and phenol red (PAA), 10% New Born Calf serum, penicillin and streptomycin. Cells were passaged every 2-3 days by resuspending in medium and seeding them to appropriate confluence. Membranes were prepared from transiently transfected HEK293T cells. One day prior to transfection 10^7 cells were seeded in a 15 cm petri dish. Cells were transfected by the addition of a 3:1 mixture of polyethyleneimine

(60µg) and plasmid DNA (20µg) in 2 mL serum free medium. The medium was refreshed after 24 hours, and after 72h the cells were harvested by suspending them in 20 mL medium. The suspension was centrifuged for 10 min at 1000 rpm, and the supernatant was removed. The cell pellet was stored at -80 ^{o}C until use.

Cell pellets were thawed on ice and suspended in lysis buffer A (20 mM HEPES, 2 mM DTT, 0.25 M sucrose, 1 mM $MgCl_2$, 1x protease inhibitor cocktail (Roche cOmplete EDTA free), 25U/µL Benzonase). The suspension was homogenized by polytrone (3 × 7 sec) and incubated for 30 min on ice. The suspension was subjected to ultracentrifugation (100.000 × g, 30 min, 4 ^{o}C, Beckman Coulter, Type Ti70 rotor) to yield the cytosolic fraction in the supernatant and the membrane fraction as a pellet. The pellet was resuspended in lysis buffer B (20 mM HEPES, 2 mM DTT, 1x protease inhibitor cocktail (Roche cOmplete EDTA free)). The protein concentration was determined with Quick Start Bradford assay (Biorad). The protein fractions were diluted to a total protein concentration of 1 mg/mL and stored in small aliquots at -80 ^{o}C until use.

PNP-butyrate DAGL activity assay. The para-nitrophenylbutyrate (PNP-butyrate) substrate assay was performed with hDAGLα as reported previously (2). In brief, this assay is based on the hydrolysis of PNP-butyrate by membrane preparations from HEK293T cells transiently transfected with hDAGLα. Reactions were performed in 50 mM pH 7.2 HEPES buffer with 0.05 µg/µL final protein concentration to which PNP-butyrate substrate was added (5.0 µL in DMSO) to a final substrate concentration of 300 µM. For the progression curve, after 135 minutes, another equal amount of substrate (5.0 µL, 12 mM) was added.

Natural substrate-based fluorescence assay (DAGLα/β). The natural DAG substrate assay was performed as reported previously (9). Standard assay conditions: 0.2 U/mL glycerol kinase (GK), glycerol-3-phosphate oxidase (GPO) and horseradish peroxidase (HRP), 0.125 mM ATP, 10 µM Amplifu™Red, 5% DMSO in a total volume of 200 µL. The assay additionally contained 5 µg/mL MAGL-overexpressing membranes, 100 µM SAG and 0.0075% (w/v) Triton X-100, with a final protein concentration of 50 µg/mL. The mDAGLβ assay was performed as the hDAGLα assay, but assay buffer was supplemented with 5 mM $CaCl_2$ and the SAG concentration was 75 µM.

Activity based protein profiling on transiently transfected HEK293T cells. HEK293T cells were transfected with hDAGLα-FLAG or hDAGLα-S472A-FLAG, hDAGLβ-FLAG or hDAGLβ-S443A-FLAG and the membranes were isolated following a protocol reported previously(2). For DAGLα ABPP assays the membrane proteome (1 mg/mL, 20 µL) was incubated at rt with vehicle (DMSO) or inhibitor in 0.5 µL DMSO for 30 min. The sample was subsequently treated for 15 min with 1µM (final concentration) ABP DH379 or 500 nM (final concentration) TAMRA-FP. The reactions were quenched with 10 µL 3 × Laemmli sample buffer (final concentrations: 60 mM Tris-Cl pH 6.8, 2% (w/v) SDS, 10% (v/v) glycerol, 5% (v/v) β-mercaptoethanol, 0.01% (v/v) bromophenol blue). The samples were directly loaded and resolved on SDS page gel (10 % acrylamide). The gels were scanned using a ChemiDoc MP system (Cy3 settings, 605/50 filter).

Western blot. Western blot procedure was performed as reported previously(2). In brief, proteins were transferred from gel to a polyvinyldifluoride membrane using a Trans-Blot® Turbo (BioRad). FLAG-tagged enzymes were stained using rabbit anti-FLAG as primary antibody, and goat-anti-rabbit HRP as secondary antibody. The blot was developed in the

dark using a 10 mL luminal solution, 100 µL ECL enhancer and 3 µL H_2O_2. Chemiluminescence was visualized using a ChemiDoc XRS (BioRad).

Size exclusion experiment Membrane proteome (1 mg/mL, 343 µL) from transfected HEK293T cells was incubated with DMSO or inhibitor in 7.0 µL DMSO for 30 min at r.t. and subsequently the protein-inhibitor complex was loaded on the size exclusion column (Zeba spin desalting columns, 2 mL). After centrifugation (1000g, 2 min) the sample was collected, and the column flushed 3 times by centrifugation (1000g, 2 min) with 1 mL of storage buffer B (20 mM HEPES, pH 7.2; 2 mM DTT). After size exclusion, 19.5µL of protein-inhibitor complex were used to perform ABPP. The rest of the sample was reloaded onto the column, and centrifugation of sample, flushing of sample and collection of 19.5 µL of sample for ABPP, were repeated several times.

Materials for radioligand binding assa.y [^{3}H]CP55940 (specific activity 141.2 Ci/mmol) and GF-C filters were purchased from Perkin Elmer (Waltham, MA). Bicinchoninic acid (BCA) and BCA protein assay reagent were obtained from Pierce Chemical Company (Rochford, IL). The PathHunter® CHO-K1 CNR1 β-Arrestin Cell Line (catalog number 93-0959C2) and the PathHunter® CHO-K1 CNR2 β-Arrestin Cell Line (catalog number 93-0706C2), stably expressing the hCB_1 receptor (CHOK1hCB_1_bgal) or hCB_2 receptor (CHOK1hCB_2_bgal) respectively, was obtained from DiscoveRx.

Cell culture and membrane preparation. CHOK1hCB_1_bgal and CHOK1hCB_2_bgal cells were cultured in Ham's F12 Nutrient Mixture supplemented with 10% fetal calf serum, 1 mM glutamine, 50 µg/mL penicillin, 50 µg/ml streptomycin, 300 mg/mL hygromycin and 800 µg/mL geneticin in a humidified atmosphere at 37°C and 5% CO_2. Cells were subcultured twice a week at a ratio of 1:20 on 10-cm ø plates by trypsinization. For

membrane preparation the cells were subcultured 1:10 and transferred to large 15-cm diameter plates. Membrane fractions were prepared exactly as described before(10).

[^{3}H]CP55940 radioligand binding assay. [^{3}H]CP55940 binding assays to determine the cannabinoid CB_1 and CB_2 receptor binding affinity were performed as follows: Ligands of interest were incubated at 30°C for 1 hr with membrane aliquots containing 5 µg CHOK1hCB_1_bgal membrane protein or 1 µg (CHOK1hCB_2_bgal) in 100 µL assay buffer (50 mM Tris–HCl, 5 mM $MgCl_2$, 0.1% BSA, pH 7.4) with [^{3}H]CP55940 in a concentration of ~1.5 nM (CB_2 receptor) or ~3.5 nM (CB_1 receptor) per assay point. Non-specific binding was determined in the presence of 10 µM Rimonabant (CB_1 receptor) or 10 µM AM630 (CB_2 receptor). Filtration was performed on GF/C filters, presoaked for 30 min with 0.25% polyethylenimine, using a Brandel harvester. Filter-bound radioactivity was determined in a β-counter. The mean % of specific binding for CB_1 and CB_2 receptors were 36 ± 4% and 38 ± 42% for 6-12 experiments.

ABPP inhibitor activity measurements. The percentage of activity remaining was determined by measuring the integrated optical intensity of the fluorescent protein bands using image lab 4.1. The relative intensity was compared to the vehicle treated proteins, which were set to 100%. IC_{50} and IC_{80} values were determined by plotting a log(inhibitor) vs. normalized response (Variable slope) dose-response curve generated using Prism software (GraphPad).

Matings and genotyping of transgenic animals. All animal experiments were carried out in compliance with institutional animal protocols, and mice were housed on a normal 6AM/6PM light/dark phase with ad libitum access to water and food. C56Bl/6 mice were

use in all inhibitor treatment studies. DAGL$\alpha^{-/-}$ and DAGL$\beta^{-/-}$ (7) mice were generated by heterozygous matings and were in a homogeneous C57Bl/6 background. For these DAGL transgenic mice PCR genotyping of genomic tail DNA was performed using the following primers: DAGLα 5'-tgagattggtatcaagacctttg-3', 5'-ccttgctcctgccgagaaagtatcc-3', and 5'-gaagaacaggtaaccaggaccat-3' (300-bp product in wild-type mice, 600-bp product in mice with the DAGLα null allele); DAGLβ 5'-aaggaggcaaagacagcaaagtgc-3', 5'-tatcctaggtgcagacagattgtgc-3', and 5'-aaatggcgttacttaagctagcttgc-3' (390-bp product in wild-type mice, 195-bp product in mice with the DAGLβ null allele).

Preparation of tissue proteomes. Mouse tissues were dounce homogenized in lysis buffer (20 mM HEPES, 250 mM sucrose, 2 mM DTT, 1 mM $MgCl_2$ with or without 25 U/mL benzonase) and incubated in ice for 5 min, followed by a low-speed spin (1,400−2.500 x g, 3 min, 4 °C) to remove debris. The membrane and cytosolic fractions were separated by ultracentrifugation (100,000 x *g*, 45 min, 4 °C) of the resulting homogenate lysate. After removal of the soluble supernatant, the membrane pellet was washed 1X with cold HEPES buffer (20 mM, with or without 2 mM DTT) followed by resuspension in cold HEPES buffer (20 mM, with or without 2 mM DTT) by pipetting. Total protein concentrations in membrane and soluble fractions were determined using the Bio-Rad DC protein assay kit. Samples were stored at -80 °C until further use.

Tissue profiling by gel-based competitive ABPP. Gel-based ABPP assays were performed as previously reported (11). Cell or tissue proteomes were treated with either FP-rhodamine (1 μM or 500 nM final concentration), HT-01 (1 μM final concentration), or DH379 (1 μM final concentration). For HT-01and DH379 labeled samples, 2 mg/mL of proteome was used to enhance endogenous DAGL signals; 1 mg/mL proteome was used

for labeling with FP-Rh. Probe labeling was carried out for 30 min at r.t. or 37 °C followed by addition of 4X SDS-PAGE loading buffer to quench the reaction. After separation by SDS-PAGE (10% acrylamide), samples were visualized by in-gel fluorescence scanning using a ChemiDoc MP system.

Copper-catalyzed azide-alkyne cycloaddition (CuAAC or click) chemistry-ABPP. Mouse brain membrane proteomes from either naïve (in vitro) or inhibitor-treated (in vivo) mice were prepared for analysis as described in preparation of tissue proteome. Using previously developed methods (12), Cyanine 5-Azide (Cy5−N_3) was conjugated to each alkyne probe for in-gel analysis. Briefly, $CuSO_4$ (1.0 µL/reaction, 100 mM in H_2O), THPTA (0.2 µL/reaction, 100 mM in H_2O), sodium ascorbate (0.6 µL/reaction, 1 M in H_2O [freshly prepared]), and Cy5−N_3 (0.2 µL/reaction, 0.4 mM in DMSO) were premixed. This click reagent mixture (2.0 µL total volume) was immediately added to each proteome (18 µL), and the reaction was stirred by briefly vortexing. After 30 min at room temperature, reactions were diluted with 4×SDS loading buffer (10 µL) and resolved by SDS-PAGE.

In vivo studies with DO34, DH376 and DO53. The animal experiments were conducted in accordance with the guidelines of the Institutional Animal Care and Use Committee of The Scripps Research Institute and the ethical committee of Leiden University (DEC#14137). In vivo studies with DO34, DH376 and DO53 were conducted in C57BL/6 mice. Mice were injected with DO34, DH376 and DO53 i.p. in 18:1:1 (v/v/v) solution of saline/ethanol/PEG40 (ethoxylated castor oil, 10 µL/g body weight of mouse). For dose-response studies, mice were treated with varying doses of compounds for 4 h, anesthetized with isoflurane, and euthanized by cervical dislocation. For time-course studies, mice were treated with 50 mg/kg body weight of compound and euthanized after

the indicated times. LPS-induced neuroinflammation studies were performed as previously described (13). Mice were pretreated with compounds i.p. in vehicle of 18:1:1 (v/v/v) solution of saline/ethanol/PEG40 (ethoxylated castor oil, 10 µL/g body weight of mouse) and incubated for 1-1.5 h. After the pretreatment, mice were treated with 20 mg/kg body weight of LPS i.p. in saline (10 µl/g body weight of mouse) and euthanized after 6 h.

Sample preparation and targeted LC/MS metabolite profiling. Mice were anesthetized by isoflurane and euthanized by decapitation. Brain tissues were harvested, and immediately frozen in liquid nitrogen. Tissues were then dounce-homogenized in 8 ml of 2:1:1 $CHCl_3$/MeOH/PBS containing the internal standard mix (1 nmol of 2-arachidonoylglycerol-d5 (2-AG-d_5), arachidonic acid-d8 (AA-d_8), anandamide-d5 (AEA-d_4), 1-stearoyl-2-arachidonoyl-sn-glycerol-d8 (SAG-d_8), prostaglandin E2-d9 (PGE2-d_9) (Cayman Chemical), 1-heptadecanoyl-2-hydroxy-sn-glycero-3-phosphocholine (LysoPC), 1,2-diheptadecanoyl-sn-glycero-3-phosphocholine (PC), 1,2-diheptadecanoyl-sn-glycero-3-phosphoethanolamine (PE), 1-(10Z-heptadecenoyl)-2-hydroxy-sn-glycero-3-[phosphor-L-serine] (LysoPS), 1,2-diheptadecanoyl-sn-glycero-3-phospho-L-serine (PS), 1,2-diheptadecanoyl-sn-glycero-3-[phosphor-rac-(1-glycerol)] (PG), 1-heptadecanoyl-2-arachidonoyl-sn-glycero-3-phospho(1'-myo-inositol) (PI) (Avanti Polar Lipids) and 1,2-dioleoyl-sn-glycero-3-phospho (N-nonadecenoyl) ethanolamine (14) (NAPE)). Homogenates were centrifuged at 1,400 x *g* for 3 min to separate the two phases. The organic phase (bottom) was removed, 20 µL of formic acid was added to acidify the aqueous homogenate and $CHCl_3$ was added to make up 8 mL volume. The mixture was vortexed and separated using centrifugation as described above. Both the organic extracts were pooled and dried under a stream of N_2. The metabolomes were resolubilized in 480 µL of 2:1 $CHCl_3$/MeOH, and 10 µL were used for the targeted LC/MS analysis.

Metabolites analyzed in this study were quantified using LC/MS–based multiple reaction monitoring (MRM) methods (Agilent Technologies 6460 Triple Quad). Liquid chromatography (LC) separation was achieved using a Gemini reverse-phase C18 column (50 x 4.6 mm with 5 μm diameter particles, Phenomonex) along with a pre-column (C18, 3.5 μm, 2 mm x 20 mm). For analysis of diacylglycerols (DAGs) and triacylglycerols (TAGs), a Luna C5 column (50 x 4.60 mm with 5 μm diameter particles) was used. Mobile phase A was made of 95:5 (v/v) H_2O:MeOH, and mobile phase B was composed of 60:35:5 (v/v/v) *i*-PrOH:MeOH:H_2O. Ammonium hydroxide (0.1%) and formic acid (0.1%) was included to assist in ion formation in negative and positive ionization modes, respectively. For analysis of DAGs and TAGs, 5 mM ammonium formate was also used in addition to 0.1% formic acid to assist in positive ionization and NH_4^+ adduct formation. MS analysis was performed with an ESI source in scanning mode from *m/z* = 50 – 1,200, capillary voltage set to 3.5 kV, and the fragmentor voltage set to 100 V. The drying gas temperature was set to 300 °C, drying gas flow rate was 11 L/min, and nebulizer pressure was 35 psi. The parameters (MS) used for MRM to measure the indicated metabolites are summarized in **Dataset S2**. Endogenous lipids were quantified by measuring the area under the peak in comparison with the appropriate unnatural internal standard and normalizing for tissue weight.

ABPP-reductive dimethylation (ReDiMe) sample preparation and analysis. For the ABPP-ReDiMe samples, proteomes (2 mg/mLin 20 mM HEPES buffer) were labeled with FP-biotin (10 μM) for 1 h at rt. After labeling, the proteomes were denatured and precipitated using 4:1 MeOH/$CHCl_3$, resuspended in 0.5 ml of 6 M urea in PBS with 0.4% SDS, reduced using Tris(2-carboxyethyl)phosphine (TCEP, 20 mM)/K_2CO_3 (60 mM) for 30 min at 37 °C and then alkylated using iodoacetamide (40 mM) for 30 min at 25 °C in the

dark. The biotinylated proteins were enriched with PBS-washed streptavidn-agarose beads (100 µL; Thermo) by shaking at rt for 1.5 h in PBS with 2% SDS to final volume of 5.5 ml. The beads were washed sequentially with 15 mL PBS with 1% SDS (3×), 15 mLPBS (3×) and 15 mL DI H_2O (3×). On-bead digestion was performed using sequence-grade trypsin (1.5 µg; Promega) in 2 M urea in triethylammonium bicarbonate buffer (100 mM, 200 µL) with 1 mM $CaCl_2$ for 12–16 h at 37 °C with constant shaking. Reductive dimethylation was performed as previously described (15, 16). Briefly, either ^{13}C-labeled deuterated formaldehyde (heavy) or formaldehyde (light) was added to each sample (0.2%) followed by addition of sodium cyanoborohydride (27 mM). Following a 2-h incubation period at room temperature, the reaction was quenched by addition of NH_4OH (0.2 %) and formic acid (8 %). The samples were then combined and analyzed by LC/MS analysis.

MS and data analysis. MS was performed using a Orbitrap Velos mass spectrometer following previously described protocols (17, 18). Peptides were eluted using a five-step multidimensional LC/MS [MudPIT(19)] protocol (using 0%, 25%, 50%, 80% and 100% salt bumps of 500 mM aqueous ammonium acetate, followed by an increasing gradient of aqueous acetonitrile and 0.1% formic acid in each step). For all samples, data were collected in data-dependent acquisition mode over a range from 400–1,800 *m*/*z*. Each full scan was followed by up to 30 fragmentation events for experiments using Orbitrap Velos instruments. Dynamic exclusion was enabled (repeat count of 1, exclusion duration of 20 s) for all experiments. The data were searched using the ProLuCID algorithm against a mouse reverse-concatenated nonredundant (gene-centric) FASTA database that was assembled from the Uniprot database. ProLuCID searches specified static modification of cysteine residues (+57.0215 *m*/*z*; iodoacetamide alkylation) and required peptides to contain at least one tryptic terminus. Each data set was independently searched with light

and heavy parameter files; for the light search, static modifications on lysine (+ 28.0313 *m*/*z*) and N termini (+ 28.0313 *m*/*z*) were specified; for the heavy search, static modifications on lysine (+ 34.06312 *m*/*z*) and N termini (+ 34.06312 *m*/*z*) were specified. The resulting matched MS2 spectra were assembled into protein identifications, then filtered using DTASelect (version 2.0.47). Peptides were restricted to a specified false positive rate of <1%. ReDiMe ratios were quantified using in-house CIMAGE (20) software. Briefly, extracted MS1 ion chromatograms (± 10 ppm) from both 'light' and 'heavy' target peptide masses (*m/z*) were generated using a retention time window (± 10 min) centered on the time when the peptide ion was selected for MS/MS fragmentation, and subsequently identified. Next, the ratios of the peak areas under the light and heavy signals (signal-to-noise ratio > 2.5) are calculated. Computational filters used to ensure that the correct peak-pair is used for quantification include a co-elution correlation score filter (R2 ≥ 0.8), removing target peptides with bad co-elution profile, and an 'envelope correlation score' filter (R2 > 0.8) that eliminates target peptides whose predicted pattern of the isotopic envelope distribution does not match the experimentally observed high-resolution MS1 spectrum. Also, peptides detected as singletons, where only the heavy or light isotopically labeled peptide was detected and sequenced, but which passed all other filtering parameters, were given a standard ratio of 20, which is the maximum ReDiMe ratio reported here.

Cytokine measurements. Cytokines were measured using mouse DuoSet® ELISA development kit (R&D Systems). Brains were homogenized in phosphate-buffered saline with 1 x protease inhibitor cocktail (Roche). The supernatant from a 1400 x g centrifugation of the homogenate was then centrifuged at 100,000 x g for 45 min. The supernatant from this centrifugation (the mouse brain soluble proteome) was used in the assay.

Slice preparation. C57BL/6J mice of either sex were anaesthetized by isoflurane inhalation and decapitated. Parasagittal slices (250 μm thick) were cut from the cerebellar vermis of 10- to 14-day-old mice, and transverse slices (250 μm thick) were cut from the hippocampus of 20- to 30-day-old mice, as we have described (21, 22). Slices were prepared at 4-6°C in a sucrose-based solution containing (in mM): 78 NaCl, 68 sucrose, 26 $NaHCO_3$, 2.5 KCl, 1.25 NaH_2PO_4, 2 $CaCl_2$, 2 $MgCl_2$ and 25 glucose. Slices were incubated for 30-40 min in sucrose solution and then transferred and stored in the artificial cerebrospinal fluid (ACSF) containing (in mM): 119 NaCl, 2.5 KCl, 2.5 $CaCl_2$, 1 $MgCl_2$, 1.25 NaH_2PO_4, 26 $NaHCO_3$, and 10 glucose. All solutions were saturated with 95% O_2 and 5% CO_2.

Electrophysiology. Whole-cell recordings were made using patch clamp amplifier Multiclamp 700B under infrared-DIC microscopy. Data acquisition and analysis were performed using DigiData 1440A digitizer and analysis software pClamp 10 (Molecular Devices). Signals were filtered at 2 kHz and sampled at 10 kHz. Whole-cell voltage-clamp recordings were made from cerebellar Purkinje cells (PCs) and hippocampal CA1 pyramidal neurons as described previously (21, 22). Excitatory postsynaptic currents (EPSCs) were recorded from cerebellar Purkinje cells (PCs), parallel fibers (PFs) were stimulated with a bipolar tungsten stimulation electrode (WPI) that was placed in the molecular layer. PF-EPSCs showed graded responses and exhibited paired-pulse facilitation (30-50 ms intervals) (23). $GABA_A$ receptor blocker picrotoxin (50 μM) and a low concentration (1 μM) of AMPA receptor antagonist 6-cyano-7-nitroquinoxaline-2,3-dione (CNQX) was present in the ACSF. Glass pipettes (3-5 MΩ) were filled with an internal solution containing (in mM): 140 cesium methanesulfonate, 10 CsCl, 2 QX-314, 10

HEPES, 0.2 EGTA, 2 $MgCl_2$, 4 Mg-ATP, and 0.3 Na_2GTP (pH 7.2 with CsOH). EPSCs were evoked by electrical stimulation at 4 s intervals. DSE was induced by a brief depolarization (1 s from -70 mV to 0 mV).

Inhibitory postsynaptic currents (IPSCs) were recorded from CA1 pyramidal neurons in hippocampal slices. A bipolar tungsten stimulation electrode was placed in the stratum radiatum of the CA1 region to evoke IPSCs. AMPA receptor antagonist CNQX (20 μM) and NMDA receptor antagonist D-2-amino-5-phosphonovaleric acid (D-AP-5, 20 μM) were present in the ACSF. The pipettes were filled with an internal solution containing (in mM): 100 K-gluconate, 50 KCl, 0.1 $CaCl_2$, 1 EGTA-Na_4, 2 $MgCl_2$, 2 Mg-ATP, 0.3 Na_2GTP, and 10 HEPES at pH 7.2 (with KOH). To induce DSI, the CA1 pyramidal neurons were depolarized from -70 mV to 0 mV for 5 s, and IPSCs were evoked at 4 s intervals. All recordings were performed at 32 ± 1°C by using an automatic temperature controller. DAGL inhibitors and control compounds were dissolved in DMSO and the final concentration of DMSO in the ACSF is ≤0.1%.

Anapyrexia study. Core body temperature was measured by radiotelemetry as previously described(24-27). Briefly, mice were anesthetized with isofluorane (induction 3-5%, maintenance 1-1.5%) and surgically implanted with radiotelemetry devices (TA-F20, Data Sciences, St. Paul, MN) into the peritoneal cavity for core body temperature (CBT) and locomotor activity (LA) evaluation. Following surgical implantation and appropriate wound closure, the animals were allowed to recover for 2 weeks and then subjected to telemetry recordings. Mice were individually housed in a Plexiglas cage in a room maintained at 25 ± 0.5°C. The cages were positioned onto the receiver plates (RPC-1; Data Sciences) and radio signal reporting CBT and LA information from the implanted transmitter was recorded continuously with a fully automated data acquisition system (Dataquest ART, Data

Sciences, St. Paul, MN). Access to food and water was ad libitum and the light:dark cycle was of 12h:12h. Anapyrexia was induced by intraperitoneal injection of *Bacterial lipopolysaccharides (LPS)* (0127:B8, Sigma, St. Louis, MO) at a dose of 10 mg/kg in saline. DH376, DO34, DO53 were injected intraperitoneally at a dose of 50 mg/kg in emulfor:ethanol:saline 1:1:18 2 h before injection of LPS. Saline and emulfor:ethanol:saline were used as vehicle.

Data analysis and statistics. Data are shown as the mean ± SEM. A Student's t test (unpaired, two-tailed) was used to determine differences between two groups. Data that included more than two groups or two factors were analyzed by one-way or two-way ANOVA, respectively, with post hoc Sidak's multiple comparisons test. All statistical analyses were conducted using Excel or GraphPad Prism version 6, and a P value less than 0.05 was considered significant throughout unless indicated otherwise. For brain lipid profiling study for DH376-, DO34-, DO53-terated mice and DAGL$\alpha^{-/-}$ mice (**Dataset S2**), Benjamini Hochberg correction (10 % false discovery rate) was applied. Post-correction p values < 0.007 were designated as significant and are marked in red. We have also listed p values between 0.007 and 0.05 in blue, with remaining p values designated as NS (not significant). For electrophysiology data, DSE and DSI were analyzed as described in our previous studies (21, 22).

Chemistry Procedures:

Materials. All chemicals were obtained from commercial suppliers and were used without further purification. Merck silica gel TLC plates (0.25 mm, 60 F254) were used to monitor reactions. Flash chromatography was performed using SiliaFlash F60 silica gel (40–63 μm, 60 Å). NMR spectra were recorded at room temperature or at high temperature (60°C or 100 °C) on Bruker AV 400 MHz spectrometer at 400 (^{1}H) and 101 (^{13}C) MHz, or on Bruker DRX-600 spectrometer at 600 (^{1}H) and 150 (^{13}C) MHz using $CDCl_3$, CD_3OD or $(CD_3)_2SO$ as solvent, unless stated otherwise. Chemical shifts are recorded in ppm relative to tetramethylsilane (TMS) with peaks being reported as follows: chemical shift, multiplicity (s = singlet, br s = broad singlet, d = doublet, t = triplet, q = quartet, m = multiplet), coupling constant (Hz). High-resolution mass spectra (HRMS) were obtained on an Agilent LC/MSD TOF mass spectrometer by electrospray ionization–time-of-flight (ESI-TOF) or on a Thermo Scientific LTQ Orbitrap XL. HPLC purification was performed on a preparative LC-MS system (Agilent 1200 series) with an Agilent 6130 Quadruple MS detector. Optical rotations were measured on a Propol automatic polarimeter (Sodium D-line, λ = 589 nm). Asterisk in the ^{1}H-NMR spectra designates the triazole ring proton. In previous studies(3), we have found this signal to be suppressed in 1,4-regiosomeric triazole-urea compounds bearing a 2- benzyl (e.g. KT116, KT109, KT172) but not 2-phenyl (e.g. KT195) group.

Synthesis of DH376

*Scheme 1: Preparation of triazole **11**.*

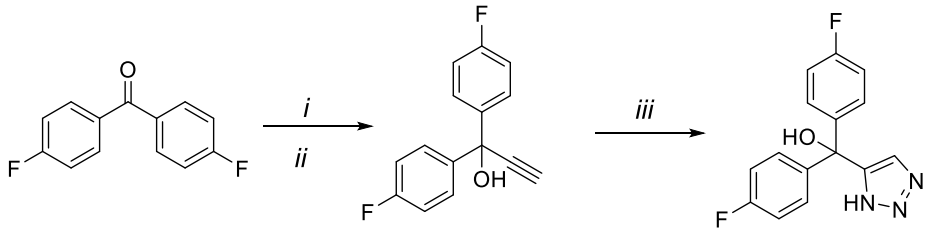

9 **10** **11**

Reagents and conditions: *i)* ethynyltrimethylsilane, n-BuLi, THF, -10 ^{o}C *ii)* NaOH, MeOH *iii)* azidotrimethylsilane, CuI, DMF/MeOH (5:1), 100 ^{o}C.

1,1-bis(4-fluorophenyl)prop-2-yn-1-ol (10): To a solution of ethynyltrimethylsilane (0.712 mL, 5.04 mmol) in anhydrous THF (20 mL) under a nitrogen atmosphere was slowly added n-butyllithium (3.15 mL, 5.04 mmol) (1.6 M in hexane) at -10°C. After stirring for one hour at -10 °C a solution of bis(4-fluorophenyl)methanone (**9**) (1.00 g, 4.58 mmol) in dry THF (10 mL) was added. After stirring for three hours at -10 °C, the temperature was raised to 0 °C and a solution of NaOH (238 mg, 5.95 mmol) in MeOH (4.60 mL) was added. The solution was warmed to room temperature, neutralized to pH 7 with acetic acid and poured into water. Subsequent extraction with ethyl acetate (3x10 mL), drying over $MgSO_4$, filtering and concentration *in vacuo* afforded a crude product that was purified by flash chromatography over silica gel using pentane/ethyl acetate, yielding **10** (1.08 g, 4.42 mmol, 96 %) as a yellow oil. ^{1}H NMR (400 MHz, $CDCl_3$) δ 7.57 – 7.51 (m, 4H), 7.03 – 6.98 (m, 4H), 2.89 (s, 2H); ^{13}C NMR (101 MHz, $CDCl_3$) δ 162.50 (d, *J* = 248 Hz), 140.24 (d, *J* = 3.1 Hz), 127.98 (d, *J* = 9.1 Hz), 115.32 (d, *J* = 21 Hz), 86.08, 76.09, 73.52; HRMS(m/z):$[M+H]^+$ calcd. for $C_{15}H_{10}F_2O$, 245.07782; found: 245.07735.

bis(4-Fluorophenyl)(1H-1,2,3-triazol-4-yl)methanol (11): 1,1-bis(4-fluorophenyl)prop-2-

yn-1-ol (**10**) (1.00 g, 4.09 mmol) and CuI (0.153 g, 0.819 mmol) were dissolved in DMF/MeOH (5:1, 36 mL). Azidotri- methylsilane (0.815 mL, 6.14 mmol) was added and the mixture was stirred at 100 °C over the weekend. The reaction mixture was quenched with H_2O (90 mL), the organic layer extracted with DCM (3 x 100 mL). The combined organic layers were washed with H_2O and brine and dried on $MgSO_4$. Filtering and concentration under reduced pressure gave a residue that was purified by flash chromatography over silica gel using pentane/ethyl acetate with 1% Et_3N (30–100% pentane/ethyl acetate) yielding **11** (0.694 g, 2.42 mmol, 59 %) as a white solid. ^{1}H NMR (400 MHz, MeOD) δ 7.58 (s, 1H), 7.38 – 7.31 (m, 4H), 7.06 – 7.01 (m, 4H); ^{13}C NMR (101 MHz, MeOD) δ 163.45 (d, *J* = 246 Hz), 143.57 (d, *J* = 2.0 Hz), 130.62, 128.59, 130.31 (d, *J* = 9.1 Hz), 115.52 (d, *J* = 22 Hz), 76.99; HRMS(m/z):$[M+H]^+$ calcd. for $C_{15}H_{11}F_2N_3O$, 288.09429; found 288.09473.

*Scheme 2: Preparation of amine **7**.*

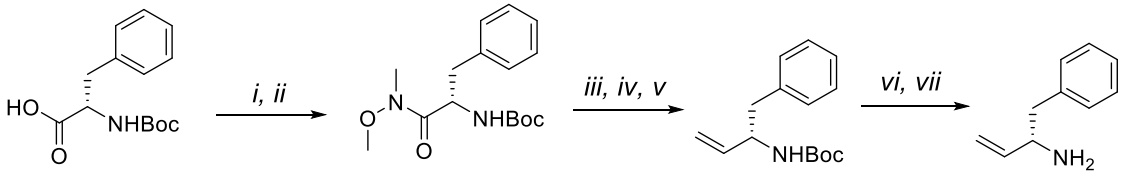

12 **13** **14** **15**

Reagents and conditions: *i)* Me(OMe)NH.HCl *ii)* EDCI, NMM *iii)* $LiAlH_4$ *iv)* H_3O^+ *v)* $(Ph)_3P{=}CH_2$ *vi)* MeOH / 6M HCl *vii)* NaOH.

(*S*)-1-phenylbut-3-en-2-amine (15): Compound **14** was prepared according the route reported(28) for the (*R*)-enantiomer on 120 mmol scale, affording 25.4 g of compound **14** (86%, $[\alpha]_D^{20}$ = +35.0 (*c* = 1.00, $CHCl_3$); Lit(28) for the (*R*)-enantiomer $[\alpha]_D^{25}$ = -37.2 (*c* =

0.28, $CHCl_3$)). The Boc-protetected amine **14** was dissolved in a mixture of MeOH (200 mL) and aqueous 6M HCl (50 mL). After TLC confirmed total conversion of compound **14** evaporation of the solvents afforded a white solid that was dissolved in water (200 mL). After addition of aqueous 8M NaOH (30 mL), extraction with chloroform (4 x 75 mL), drying ($MgSO_4$), filtering and evaporation of the solvent, amine **15** was obtained as a brown oil that was used without further purification. $[\alpha]_D^{20}$ = +14.1 (*c* = 1.00, $CHCl_3$); Lit(29) $[\alpha]_D^{25}$ = 15.1 (*c* = 1.00, $CHCl_3$); ^{1}H NMR (400 MHz, $CDCl_3$) δ 7.31 – 7.19 (m, 5H), 5.88 (ddd, *J* = 17.2, 10.3, 6.3 Hz, 1H), 5.13 (d, *J* = 17.2 Hz, 1H), 5.03 (d, *J* = 10.3 Hz, 1H), 3.59 (q, *J* = 6.3 Hz, 1H), 2.82 (dd, *J* = 13.3, 5.3 Hz, 1H), 2.61 (dd, *J* = 13.3, 8.3 Hz, 1H), 1.28 (br s, 2H); ^{13}C NMR (101 MHz, $CDCl_3$) δ 142.30, 138.65, 129.29, 128.28, 126.22, 113.52, 55.36, 44.23; HRMS(m/z):$[M+H]^+$ calcd. for $C_{10}H_{13}N$, 148.11208; found 148.11199; For chiral HPLC analysis amine **15** was derivatized as its benzoate followed by analysis on a Daicel Chiralpak AD column (250 x 4.5 mm, 10µm particle size). Eluent hexane / 2-propanol = 90 /10, 1.0 mL / min., detection UV 254 nm. (*R*)-Enantiomer, R_t = 12.2 min (not observed); (*S*)-enantiomer, R_t = 14.4 min (100%). See figure 1.

*Figure 1: Chiral HPLC analysis for N-benzoylated compound **15**.*

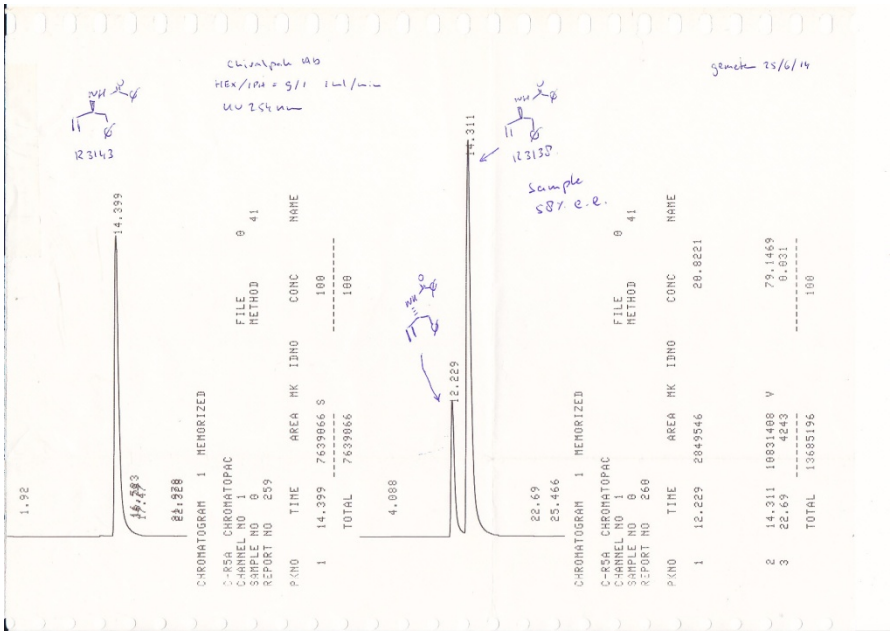
Chiralpak IA3
HEX/IPA = 9/1 1 ml/min
UV 254 nm
geneeka 25/6/14
R3143
R2138
14.399
14.311
12.229
sample
58% e.e.
1.92
4.088
22.69
25.466
CHROMATOGRAM 1 MEMORIZED
C-R5A CHROMATOPAC
CHANNEL NO 1
SAMPLE NO 0
REPORT NO 259
FILE
METHOD 0 41
PKNO TIME AREA MK IDNO CONC NAME
1 14.399 7639066 S 100
TOTAL 7639066 100
CHROMATOGRAM 1 MEMORIZED
C-R5A CHROMATOPAC
CHANNEL NO 1
SAMPLE NO 0
REPORT NO 260
FILE
METHOD 0 41
PKNO TIME AREA MK IDNO CONC NAME
1 12.229 2849546 20.8221
2 14.311 10831498 V 79.1469
3 22.69 4243 0.031
TOTAL 13685196 100

*Scheme 3: Preparation of compound **4 (DH376)**.*

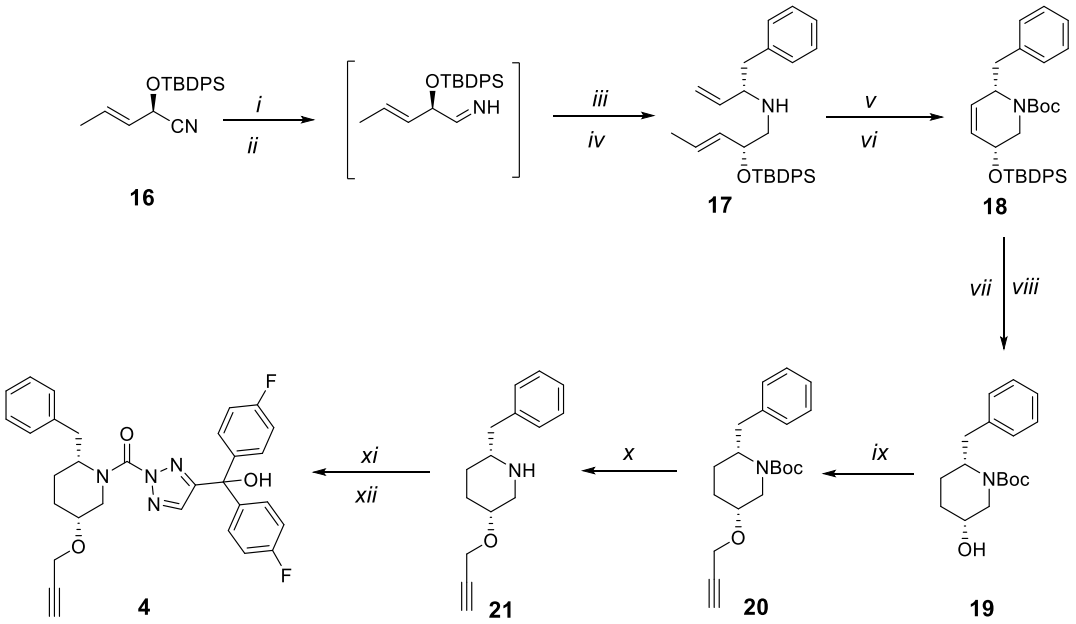

Reagents and conditions: *i)* Dibal-H, Diethyl ether, -78 ^{o}C → . *ii)* MeOH, -90 ^{o}C *iii)* amine **15** (3 eq.), MeOH *iv)* $NaBH_4$. *v)* Boc_2O, Et_3N, THF, 50 ^{o}C. *vi)* Grubbs 2nd generation, DCM, 45 ^{o}C. *vii)* TBAF, THF. *viii)* Hydrazine, $CuSO_4$, EtOH, 70 ^{o}C. *ix)* 3-bromoprop-1-yne, NaH, DMF. *x)* 20% TFA, DCM. *xi)* DIPEA, Triphosgene, THF, 0 ^{o}C. *xii)* DIPEA, DMAP, Compound **11**, THF, 60 ^{o}C.

(*R,E*)-2-((*tert*-butyldiphenylsilyl)oxy)-*N*-((*S*)-1-phenylbut-3-en-2-yl)pent-3-en-1-amine (17): Under an argon atmosphere, a flame dried three necked reaction flask was charged with a solution of (*R,E*)-2-((*tert*-butyldiphenylsilyl)oxy)pent-3-enenitrile (**16**)(30) (2.60 g, 7.76 mmol) in dry diethyl ether. At -78 °C a 1.0 M solution of Dibal-H (12.0 mL, 12.0 mmol) in toluene was added drop wise. The reaction was warmed slowly on the cooling bath until 5 °C in circa two hours. After re-cooling to -90 °C, dry MeOH (12 mL) was added at once. After five minutes followed by a solution of (*S*)-1-phenylbut-3-en-2-amine (**15**) (2.99 g, 20.3

mmol, e.e. = 99%) in MeOH (10 mL). The cooling bath was removed and the mixture stirred at room temperature for 16 hours. Subsequently, an excess of $NaBH_4$ (870 mg, 22.9 mmol) was added at 0 °C in two portions with a five minute interval. The reaction was left stirring on the ice bath and slowly warmed up to room temperature overnight. The reaction mixture was poured into an 0.8 M aqueous NaOH solution (150 mL) and extracted with diethyl ether (3 x 80 mL). The ether layers were combined and washed twice with an aqueous 1 M HCl solution (2 x 30 mL) to recover the excess (*S*)-1-phenylbut-3-en-2-amine*. The ether layers were subsequently washed with an aqueous 0.8 M NaOH-solution (50 mL) and brine (20 mL), dried ($MgSO_4$), filtered and concentrated *in vacuo* to afford the crude product as a yellow oil (3.74 g, quant.) that was used crude in the next reaction. $[\alpha]_D^{22}$ = -18.0 (*c* = 1.00, $CHCl_3$); ^{1}H NMR (400 MHz, $CDCl_3$) δ 7.64 – 7.57 (m, 4H), 7.42 – 7.27 (m, 6H), 7.23 (app. t, *J* = 7.2 Hz, 2H), 7.18 – 7.10 (m, 3H), 5.58 (ddd, *J* = 17.8, 10.3, 7.9 Hz, 1H), 5.35 – 5.26 (m, 1H), 5.23 – 5.09 (m, 1H), 5.05 – 4.90 (m, 2H), 4.16 (app. q, *J* = 5.9 Hz, 1H), 3.17 (app. q, *J* = 7.5 Hz, 1H), 2.78 – 2.62 (m, 3H), 2.38 (dd, *J* = 11.5, 5.7 Hz, 1H), 1.52 (br s, 1H), 1.42 (d, *J* = 6.4 Hz, 3H), 0.99 (s, 9H); ^{13}C NMR (101 MHz, $CDCl_3$) δ 140.75, 138.53, 135.94, 135.79, 134.24, 134.11, 132.21, 129.44, 129.32, 128.20, 127.39, 127.21, 126.16, 115.76, 74.00, 63.04, 53.64, 42.54, 26.98, 19.20, 17.45; IR (film) 3071, 2930, 2857, 1472, 1105, 1078, 1030, 964 cm^{-1}; HRMS(m/z):$[M+H]^+$ calcd. for $C_{31}H_{39}NOSi$, 470.28737; found 470.28682.

*The two combined acidic water layers from above were basified with 8 M NaOH (12 mL) and extracted with chloroform (4 x 30 mL). Drying ($MgSO_4$), filtering and concentration *in vacuo* afforded recovered amine **15** (2.03 g, (13.8 mmol).

***tert*-Butyl ((*R,E*)-2-((tert-butyldiphenylsilyl)oxy)pent-3-en-1-yl)((*S*)-1-phenylbut-3-en-**

2- yl)carbamate. The crude amine **17** from above (3.74 g, max 7.76 mmol) was dissolved in a mixture of THF (50 mL) and TEA (2 mL). Boc_2O (4.01 g, 18.3 mmol) was added and the reaction refluxed overnight. TLC analysis confirmed complete conversion of the amine and after evaporation of the solvents followed by silica gel column chromatography using pentane : ethyl acetate = 98 : 2 as the eluent afforded 4.40 g of the Boc-protected amine in circa 80% purity (contaminated with 20% Boc_2O). $[\alpha]_D^{20}$ = -39.6 (*c* = 1.00, $CHCl_3$); ^1H NMR (400 MHz, $CDCl_3$) mixture of rotamers (1:2) δ 7.72 – 7.57 (m, 4H), 7.44 – 7.33 (m, 6H), 7.27 – 7.10 (m, 3H), 7.02 (d, *J* = 7.0 Hz, 2H), 5.99 – 5.63 (m, 1H), 5.34 – 5.28 (m, 1H), 5.11 – 5.04 (m, 1H), 4.94 (d, *J* = 10.2 Hz, 1H), 4.75 (d, *J* = 17.3 Hz, 1H), 4.10 (br s, 1H), 4.01 – 3.78 (m, 1H), 3.55 – 3.09 (m, 1H), 3.03 – 2.79 (m, 1H), 2.70 – 2.65 (m, 2H), 1.52 (s, 3H), 1.41&1.34 (2 x s, 9H), 1.03 (s, 9H); ^{13}C NMR (101 MHz, $CDCl_3$) mixture of rotamers, major peaks: δ 154.85, 146.68, 138.58, 137.70, 137.38, 135.97, 135.81, 134.23, 133.92, 132.02, 129.61, 129.48, 129.17, 128.01, 127.52, 127.31, 125.99, 115.71, 79.14, 72.96, 62.28, 52.83, 38.41, 28.32, 27.35, 19.16, 17.73; IR (film) 3066, 2932, 2859, 1809, 1767, 1694, 1427, 1366, 1173, 1113, 1069 cm^{-1}; HRMS(m/z):$[M+H]^+$ calcd. for $C_{36}H_{47}NO_3Si$, 570.33980; found 570.33994.

***tert*-Butyl (3*R*,6*S*)-6-benzyl-3-((tert-butyldiphenylsilyl)oxy)-3,6-dihydropy-ridine-1(2*H*)-carboxylate (18)**: The Boc-protected diene from above (5.40 g, max 7.59 mmol) was dissolved in DCM (50 mL) and purged with argon. After the addition of Grubb's 2nd generation catalyst (190 mg, 0.224 mmol) and refluxing overnight TLC analysis confirmed complete conversion. The solvent was evaporated and the crude product purified by silica gel column chromatography using pentane : ethyl acetate = 99 : 1 → 97 : 3 as the eluent, to afford the title compound as a colorless oil (2.93 g, 72% based on nitrile **16**). $[\alpha]_D^{20}$ =

+47.8 (*c* = 1.00, $CHCl_3$); ^1H NMR (400 MHz $CDCl_3$) mixture of rotamers (1:1) δ 7.72 – 7.65 (m, 4H), 7.41– 7.34 (m, 6H), 7.30 – 7.09 (m, 5H), 5.72 – 5.64 (m, 1H), 5.52 – 5.42 (m, 1H), 4.57 – 4.38 (m, 1H), 4.38 – 3.94 (m, 2H), 2.95 – 2.84 (m, 1H), 2.80 – 2.67 (m, 2H), 1.31&1.29 (2 x s, 9H), 1.09 (s, 9H); ^{13}C NMR (101 MHz, $CDCl_3$) mixture of rotamers (1:1) δ 153.86, 153.77, 138.15, 137.88, 135.69, 135.60, 133.92, 133.73, 133.65, 133.54, 131.23, 131.13, 129.69, 129.61, 129.34, 129.27, 128.31, 128.16, 127.75, 127.60, 127.55, 126.28, 126.18, 79.55, 79.47, 65.35, 53.68, 52.66, 44.40, 42.69, 39.44, 39.09, 28.22, 28.13, 26.87, 19.11; IR (film): 3069, 3030, 2961, 2930, 2859, 1694, 1454, 1414, 1157, 1111, 1086, 1018 cm^{-1}; HRMS(m/z):$[M+H]^+$ calcd. for $C_{33}H_{41}NO_3Si$, 528.29285; found 528.29227.

***tert*-Butyl (2*R*,5*R*)-2-benzyl-5-hydroxypiperidine-1-carboxylate (19)**: A 1M solution of TBAF (2.84 mL, 2.84 mmol) in THF was added to an ice cold solution of Compound **18** (1.01 g, 1.90 mmol) in THF (15mL). After 15 minutes the cooling bath was removed and the mixture was stirred at room temperature for 2.5 h. After being diluted with water (25 mL), the mixture was extracted with ethyl acetate (3 x 20 mL), the combined organic layer was washed with water and brine, dried over $MgSO_4$ and concentrated under reduced pressure. A suspension of the above crude product (600 mg, 2.07 mmol) and $CuSO_4$ (3.31 g, 20.7 mmol) in EtOH (15 mL) was cooled on an ice bath. Hydrazine monohydrate (6.51 ml, 207 mmol) was added drop wise, the mixture was subsequently stirred for 15 minutes at room temperature and then at 70 ^oC overnight. The reaction mixture was filtered over celite and concentrated under reduced pressure. The residue was purified by flash silica gel chromatography (10-50% ethyl acetate/pentane) to furnish **19** (435 mg, 1.49 mmol, 72%) as a yellow oil. $[\alpha]_D^{22}$ = -45.7 (*c* = 0.70, $CHCl_3$). ^1H NMR (400 MHz, $CDCl_3$) δ 7.30 – 7.23 (m, 2H), 7.21 – 7.13 (m, 3H), 4.35 (br s, 1H), 4.25 (br s, 1H), 3.97 (br s, 1H), 3.63 –

3.57 (m, 1H), 2.91 (dd, *J* = 12.7, 8.2 Hz, 1H), 2.78 – 2.72 (m, 2H), 1.95 – 1.85 (m, 1H), 1.68 – 1.54 (m, 3H), 1.30 (s, 9H); ^{13}C NMR (101 MHz, $CDCl_3$) δ 154.56, 138.79, 128.98, 128.21, 126.03, 79.48, 66.76, 51.71, 45.12, 35.62, 28.24, 28.04, 26.22; HRMS(m/z):$[M+H]^+$ calcd. for $C_{17}H_{25}NO_3$, 292.19072; found 292.19080.

***tert*-Butyl (2*R*,5*R*)-2-benzyl-5-(prop-2-yn-1-yloxy)piperidine-1-carboxylate (20)**: To a solution of compound **19** (130 mg, 0.446 mmol) in DMF (3 mL) at 0 °C, was added NaH (44.6 mg, 1.12 mmol). After 5 minutes followed by drop wise addition of 3-bromoprop-1-yne (0.144 mL, 1.34 mmol). The reaction was allowed to warm to room temperature and stirred for 24 hours. The mixture was diluted with water (10 mL), and extracted with ethyl acetate (3 x 20 mL). The organic layer was washed with water, brine, dried over $MgSO_4$, filtered, and concentrated under reduced pressure. The residue was purified by flash chromatography (5-20% ethyl acetate/pentane) to furnish **20** (128 mg, 0.389 mmol, 87 %) as a yellow oil. $[\alpha]_D^{22}$ = -24.9 (*c* = 1.00, $CHCl_3$); ^{1}H NMR (400 MHz, $CDCl_3$) δ 7.29 – 7.25 (m, 2H), 7.20 – 7.16 (m, 3H), 4.42 (br s, 1H), 4.32 (br s, 1H), 4.22 (s, 2H), 3.50 – 3.45 (m, 1H), 2.88 (dd, *J* = 13.5, 7.9 Hz, 1H), 2.76 – 2.70 (m, 2H), 2.46 (t, *J* = 4.0 Hz, 1H), 2.00 – 1.93 (m, 1H), 1.66 – 1.57 (m, 3H), 1.28 (s, 9H). ^{13}C NMR (101 MHz, $CDCl_3$) δ 154.71, 138.96, 129.24, 128.51, 126.34, 80.03, 79.71, 74.43, 74.07, 56.02, 52.14, 42.15, 35.90, 28.31, 25.85; HRMS(m/z):$[M+H]^+$ calcd. for $C_{20}H_{27}NO_3$, 330.20637; found 330.20643.

(2*R*,5*R*)-2-benzyl-5-(prop-2-yn-1-yloxy)piperidine (21): To a solution of compound **20** (140 mg, 0.425 mmol) in DCM (2 mL) was added 20% TFA/DCM (5 mL), the reaction mixture was stirred at room temperature for 2.5 hours, after which TLC showed complete conversion of the starting material. Toluene (20 mL) was added and the mixture

concentrated. The mixture was dissolved in toluene (2x20 mL) two times more and concentrated *in vacuo*. The residue was diluted with ethyl acetate and washed subsequently with aqueous 10% Na_2CO_3 solution, water, brine and dried over $MgSO_4$. Filtering and concentration under reduced pressure afforded the crude product **21** that was used without further purification. ^{1}H NMR (400 MHz, $CDCl_3$) δ 7.31 – 7.26 (m, 2H), 7.23 (d, *J* = 6.9 Hz, 1H), 7.18 (d, *J* = 6.9 Hz, 2H), 4.21 (s, 2H), 4.03 (s, 1H), 3.45 (d, *J* = 12.7 Hz, 1H), 3.29 (br s, 1H), 3.17 (dd, *J* = 12.9, 4.1 Hz, 2H), 3.06 (d, *J* = 11.5 Hz, 1H), 2.85 (dd, *J* = 12.9, 9.7 Hz, 1H), 2.41 (t, *J* = 2.1 Hz, 1H), 2.05 (d, *J* = 13.3 Hz, 1H), 1.92 – 1.77 (m, 1H), 1.62 (d, *J* = 11.9 Hz, 1H), 1.51 (t, *J* = 13.3 Hz, 1H), 1.26 (br s, 1H). ^{13}C NMR (101 MHz, $CDCl_3$) δ135.40, 129.45, 128.87, 127.28, 78.87, 75.31, 66.94, 57.89, 55.32, 47.04, 39.54, 25.91, 22.66. LC-MS (m/z) :$[M+H]^+$ calcd. for $C_{15}H_{19}NO$, 230.32; found 230.10.

((2R,5R)-2-benzyl-5-(prop-2-yn-1-yloxy)piperidin-1-yl)(4-(bis(4-fluorophenyl)(hydroxy)methyl)-2H-1,2,3-triazol-2-yl)methanone (4, DH376): An ice cold solution of compound **21** (80 mg, 0.349 mmol) in THF (4 mL) was treated with DIPEA (0.305 mL, 1.74 mmol) and triphosgene (51.8 mg, 0.174 mmol) and the reaction mixture was stirred for 30 min at 0 ^oC. The mixture was poured into water and extracted with ethyl acetate (3 x 20 mL). The organic layer was washed with water, brine, dried over $MgSO_4$, filtered and concentrated under reduced pressure. The intermediate was dissolved in a mixture of THF (8 mL) and DIPEA (0.305 mL, 1.74 mmol). Subsequently DMAP (42.6 mg, 0.349 mmol) and compound **11** (100 mg, 0.349 mmol) were added to the solution. The mixture was stirred for two hours at 60 ^oC and poured into a saturated aqueous NH_4Cl solution. The mixture was extracted with ethyl acetate (3 x 20 mL), washed with water, brine, dried over $MgSO_4$, filtered. The solvents were removed under reduced pressure to

yield the crude triazole urea **4** as a mixture of *N2*- and *N1*-carbamoylated regioisomers. Regioisomers were easily distinguishable by ^{1}H-NMR shift of the triazole ring proton by comparison to NMRs for urea triazoles of known regiochemistry based on solved crystal structures(3, 31). The *N2*-carbamoyl triazole was isolated by silica gel chromatography (2-20% ethyl acetate/pentane) to afford 2,4-triazole urea (**4**, **DH376**) (47.3 mg, 0.087 mmol, 25%) as lower TLC spot. $[\alpha]_D^{22}$ = -5.16 (*c* = 1.00, $CHCl_3$); ^{1}H NMR (400 MHz, $(CD_3)_2SO$, 110 ^{o}C) δ 7.90 (s, 1H), 7.39 – 7.35 (m, 4H), 7.23 – 7.16 (m, 3H), 7.13 – 7.07 (m, 5H), 6.64 (br d, *J* = 4.0 Hz, 1H), 4.38 (br s, 1H), 4.16 (d, *J* = 2.4 Hz, 2H), 4.05 (br d, *J* = 12.0 Hz, 1H), 3.62 – 3.55 (m, 1H), 3.15 (br d, *J* = 4.0 Hz, 1H), 3.08 – 2.97 (m, 3H), 2.01 – 1.96 (m, 1H), 1.76 – 1.63 (m, 3H); ^{13}C NMR (101 MHz, $CDCl_3$, 60 ^{o}C) δ 162.57 (d, *J* = 247 Hz), 155.76, 149.37, 140.95 (d, *J* = 3.0 Hz), 137.67, 135.22, 129.96, 129.20 (d, *J* = 8.1 Hz), 128.83, 126.94, 115.28 (d, *J* = 22 Hz), 79.88, 76.69, 74.77, 73.61, 56.26, 55.17, 45.94, 36.10, 25.99, 25.88; IR (film) : 3425, 2925, 1709, 1602, 1506, 1429, 1225, 1159, 1093 cm^{-1}; HRMS(m/z):$[M+H]^{+}$ calcd. for $C_{31}H_{28}F_2N_4O_3$, 543.21575; found 543.21552.

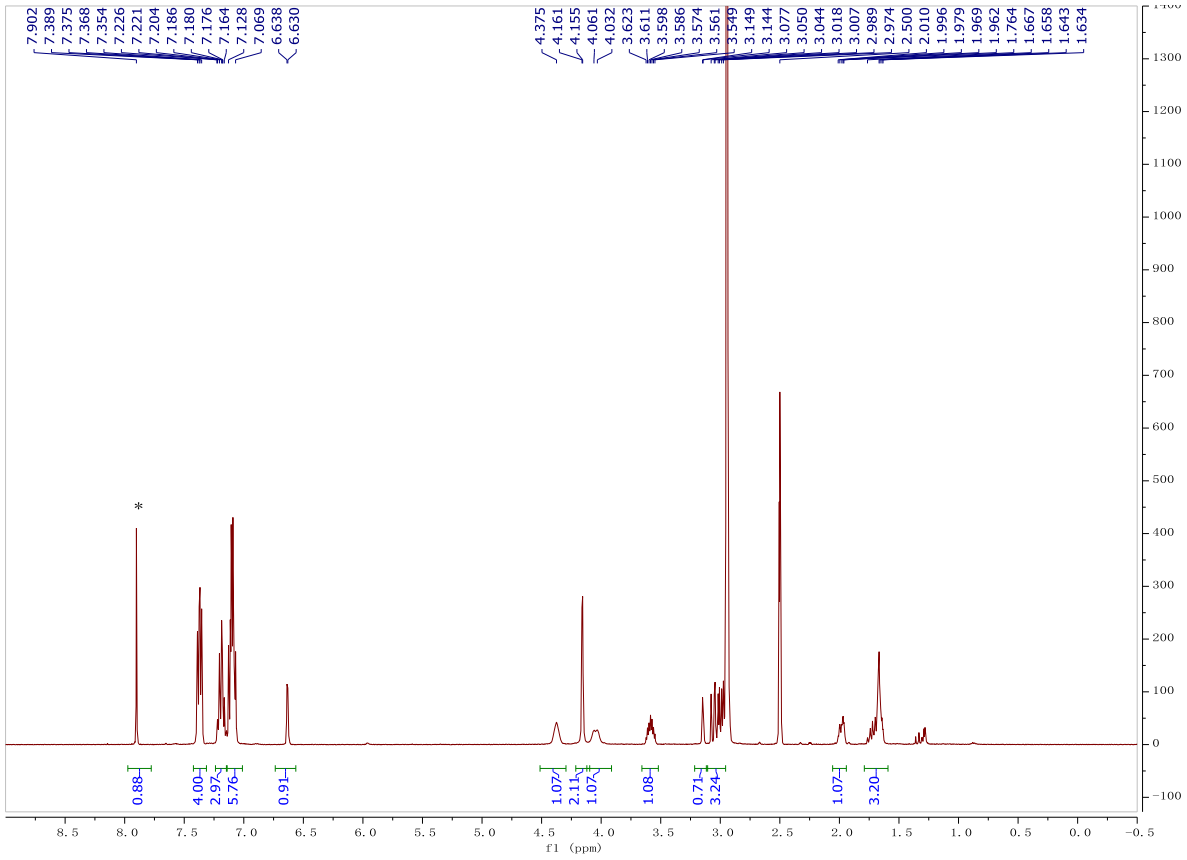
7.902
7.389
7.375
7.368
7.354
7.226
7.221
7.204
7.186
7.180
7.176
7.164
7.128
7.069
6.638
6.630
4.375
4.161
4.155
4.061
4.032
3.623
3.611
3.598
3.586
3.574
3.561
3.549
3.149
3.144
3.077
3.050
3.044
3.018
3.007
2.989
2.974
2.500
2.010
1.996
1.979
1.969
1.962
1.764
1.667
1.658
1.643
1.634
*
0.88
4.00
2.97
5.76
0.91
1.07
2.11
1.07
1.08
0.71
3.24
1.07
3.20
f1 (ppm)

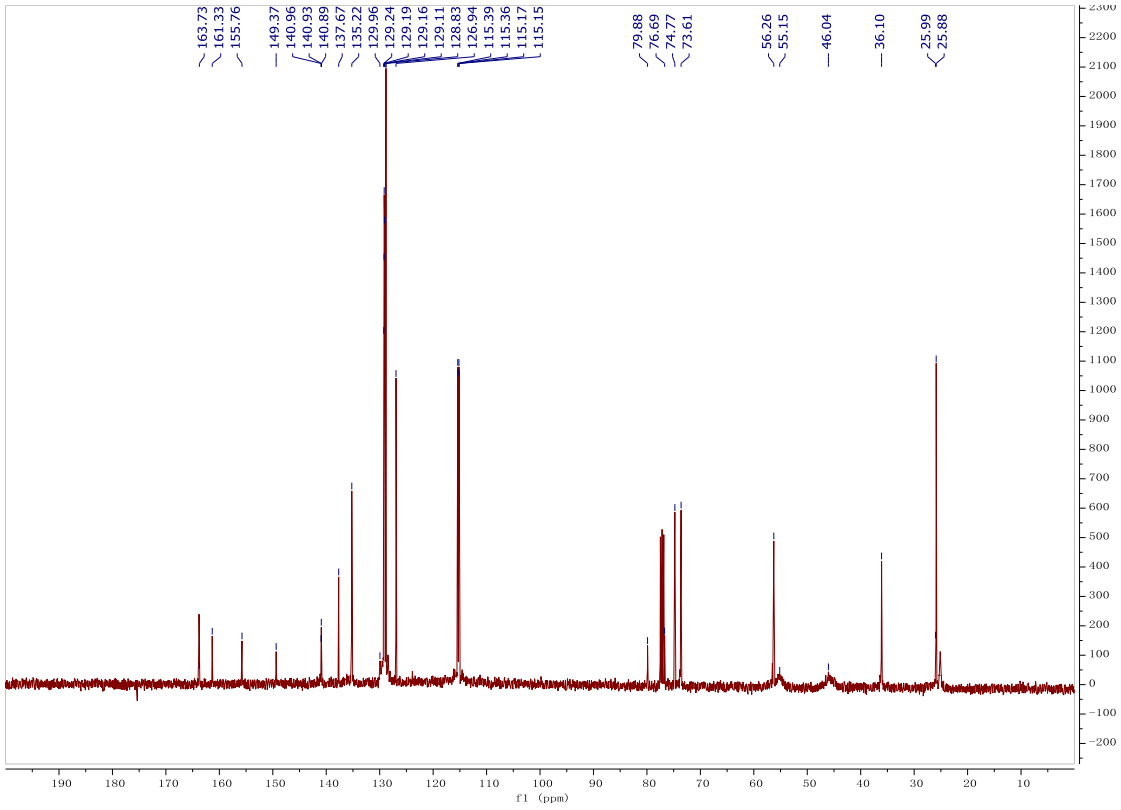

*Scheme 4: Coupling of Bodipy-azide **22** to compound **4** (DH376).*

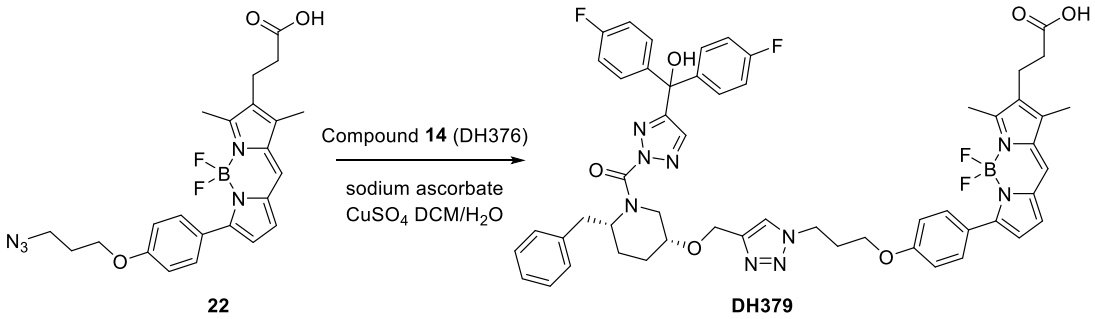

ABP-DH379: Bodipy-Azide **22**(32) (14.2 mg, 0.030 mmol) and **DH376** (15.0 mg, 0.028 mmol), were dissolved in degassed DCM/H_2O (1:1, 2 mL) and sodium ascorbate (6.57 mg,

0.033 mmol) and $CuSO_4$ (3.45 mg, 0.014 mmol) were added. The resulting mixture was stirred vigorously for two hours, after which TLC indicated completed conversion of the reaction. The solvents were evaporated *in vacuo* and the residue was taken up in DCM and purified by silica gel column chromatography (ethyl acetate with 1% AcOH) yielding probe **DH379** (9.0 mg, 0.009 mmol, 32%) as a purple solid. ^{1}H NMR (600 MHz, $CDCl_3$) δ 7.85 (br s, 2H), 7.43 (br s, 11H), 7.09 – 6.91 (m, 8H), 6.51 (br s, 1H), 4.73 (br s, 2H), 3.94 (br s, 2H), 3.67 (br s, 1H), 3.53 (br s, 1H), 3.04 (br s, 2H), 2.74 (br s, 3H), 2.51 (br s, 5H), 2.21 (br s, 3H), 1.72 (br s, 3H), 1.25 (br s, 5H), 0.92 – 0.84 (m, 2H); ^{13}C NMR (151 MHz, $CDCl_3$) δ 176.20, 162.81 (d, *J* = 242 Hz), 159.61, 159.12, 155.38, 148.95, 141.55, 141.14, 140.72, 140.16, 137.78, 135.10, 134.51, 130.94, 130.05, 129.56, 129.24, 128.76, 128.14, 126.84, 126.22, 123.23, 118.45, 115.19 (d, *J* = 18 Hz), 114.25, 76.24, 73.67, 64.09, 54.22, 51.04, 48.95, 46.61, 35.69, 29.84, 26.55, 24.64, 22.83, 14.27, 13.34, 9.83; HRMS(m/z):$[M+H]^+$ calcd. for $C_{54}H_{52}BF_4N_9O_6$, 1010.41515; found 1010.41550.

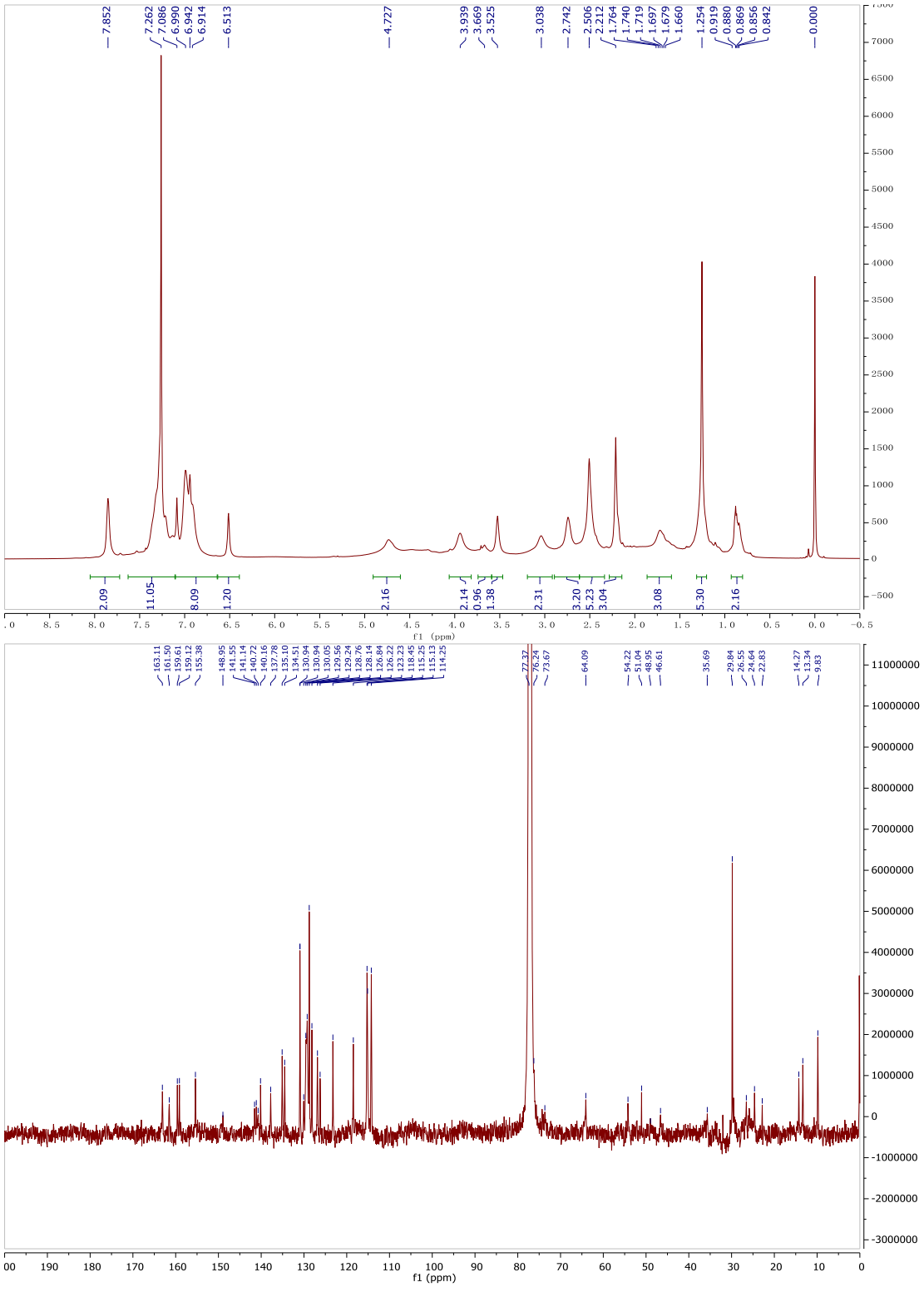
7.852
7.262
7.086
6.990
6.942
6.914
6.513
4.727
3.939
3.669
3.525
3.038
2.742
2.506
2.212
1.764
1.740
1.719
1.697
1.679
1.660
1.254
0.919
0.880
0.869
0.856
0.842
0.000
2.09
11.05
8.09
1.20
2.16
2.14
0.96
1.38
2.31
3.20
5.23
3.04
3.08
5.30
2.16
f1 (ppm)
163.11
161.50
159.61
159.12
155.38
148.95
141.55
141.14
140.72
140.16
137.78
135.10
134.51
130.94
130.64
130.05
129.56
129.24
128.76
128.14
126.84
126.22
123.23
118.45
115.25
115.13
114.25
77.37
76.24
73.67
64.09
54.22
51.04
48.95
46.61
35.69
29.84
26.55
24.64
22.83
14.27
13.34
9.83
f1 (ppm)

Synthesis of DO6, DO13, DO34 and DO53

Synthesis of (2-benzylpyperadinyl)(4-{4-(2,4,6-trimethoxy)phenyl]phenyl}-1H-1,2,3-triazol-1-yl)metanone (2, DO6)

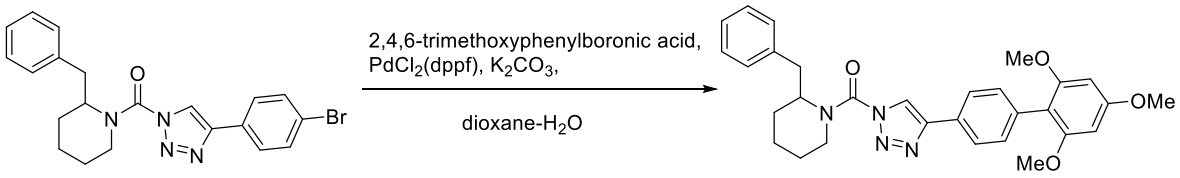

KT116 (23) DO6 (2)

KT116 was prepared as described before(7, 33). A solution of KT116 (20 mg, 0.047 mmol), 2,4,6-trimethoxyphenylboronic acid (28 mg, 0.13 mmol), K_2CO_3 (20 mg, 0.15 mmol) and $PdCl_2$(dppf) (12 mg, 0.014 mmol) in dioxane (1 mL) and H_2O (0.1 mL) was sealed in a vessel and heated in the microwave at 100 °C for 1 h. The mixture was poured into H_2O and extracted with ethyl acetate. The organic layer was washed with H_2O and brine, dried over Na_2SO_4 and concentrated under reduced pressure. The residue was purified by pTLC (ethylacetate:hexane=1:2) to afford **DO6** (**2**) (14 mg, 59%.).

H NMR ($CDCl_3$, 600 MHz) δ 7.84 (s, 2H), 7.51 (s, 1H), 7.45 (d, 2H, *J* = 7.8 Hz), 7.25 (br s, 3H), 7.04 (br s, 1H), 6.28 (s, 2H), 4.91 (s, 1H), 4.39 (1H, d, *J* = 6.3 Hz), 3.90 (s, 3H), 3.78 (s, 6H), 3.38−3.26 (m, 2H), 2.74 (br s, 1H), 2.07−1.66 (m, 6H). ^{13}C NMR ($CDCl_3$, 150 MHz) 160.89, 158.56, 149.56, 146.89, 138.13, 134.73, 131.99, 129.35, 128.92, 127.92, 126.83, 125.34, 120.53, 112.03, 91.14, 57.58, 56.11, 55.60, 43.88, 41.07, 36.76, 28.99, 25.63, 19.08. HRMS calculated for $C_{30}H_{32}N_4O_4$ $[M+H]^+$ 513.2496, found 513.2495.

Synthesis of (2-benzylpyperadinyl)(4-{4-(2,6-methoxy)pyridyl]phenyl}-1H-1,2,3-triazol-1-yl)metanone (3, DO13)

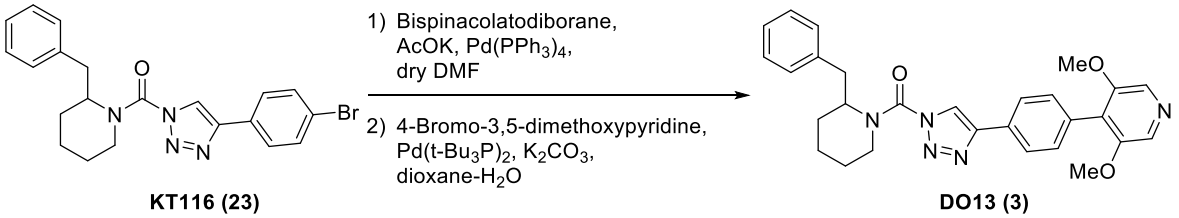

KT116 (23) DO13 (3)

A solution of KT116 (55 mg, 0.13 mmol), bispinacolatodiborane (85 mg, 0.33 mmol), AcOK (39 mg, 0.40 mmol) and $Pd(PPh_3)_4$ (40 mg, 0.036 mmol) in dry DMF (1.7 mL) was sealed in a vessel and heated in the microwave at 100 °C for 1 h. The mixture was diluted with AcOEt, washed with sat. NH_4Cl and brine, dried over Na_2SO_4 and concentrated under reduced pressure. The residue was passed through a short column (ethyl acetate:hexane=1:5) to give the crude pinacolatoborane. Resulting crude, 4-bromo-3,5-dimethoxypyridine (32 mg, 0.15 mmol), K_2CO_3 (27 mg, 0.19 mmol) and $Pd(t\text{-}Bu_3P)_2$ (15 mg, 0.029 mmol) in dioxane-H_2O was sealed in a vessel and heated in the microwave at 100 °C for 1 h. The mixture was diluted with AcOEt, washed with sat. NH_4Cl, H_2O and brine, dried over Na_2SO_4 and concentrated under reduced pressure. The residue was purified by flush column chromatography (ethyl acetate:hexane=1:1 to 3:1) to afford **DO13** (**3**) (24 mg, 38%).

^{1}H NMR ($CDCl_3$, 600 MHz) δ 8.12 (s, 2H), 7.84 (br s, 2H), 7.45 (d, 2H, *J* = 8.4 Hz), 7.20 (br s, 3H), 6.99 (br s, 1H), 4.85 (br s, 1H), 4.34 (d, 1H, *J* = 13.2 Hz), 3.85 (s, 6H), 3.34−2.22 (m, 2H), 2.69 8 (br s, 1H), 2.10−1.60 (m, 6H). ^{13}C NMR ($CDCl_3$, 150 MHz) 152.53, 148.81, 145.77, 137.48, 131.13, 130.52, 128.72, 128.27, 127.57, 126.17, 125.51, 125.20, 120.18, 56.88, 56.29, 43.33, 40.72, 36.18, 35.57, 28.18, 25.04, 18.35. HRMS calculated for $C_{28}H_{29}N_5O_3$ $[M+H]^+$ 484.2343, found 484.2344.

Synthesis of (2-benzyl-4-{[(2-methyl-2-propanyl)oxy]carbonyl}pyperazinyl){4-[(4-trifluoromethoxy)phenyl]-1H-1,2,3-triazol-1-yl}metanone (5, DO34)

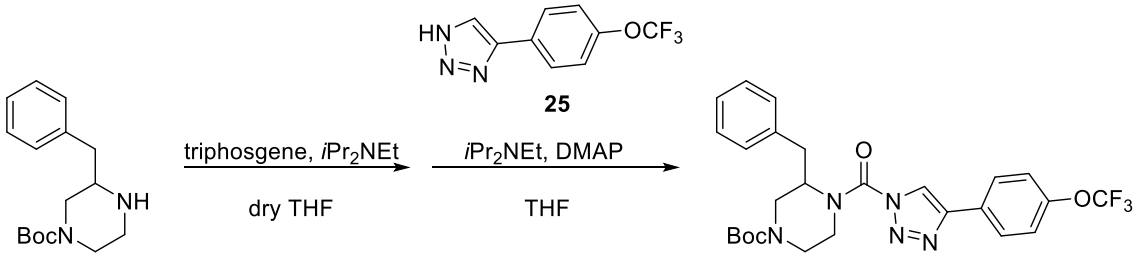

A solution of 1-Boc-3-benzylpiperazine (350 mg, 1.3 mmol) (**24**) in dry THF (9.5 mL) was treated with *i*Pr_2NEt (670 µL, 3.7 mmol) and triphosgene (190 mg, 0.63 mmol), and the reaction mixture was stirred for 30 min at 4 °C. The mixture was poured into H_2O and extracted with ethyl acetate. The organic layer was washed with H_2O and brine, dried over Na_2SO_4 and concentrated under reduced pressure. The residue was dissolved in THF (20 mL), and *i*Pr_2NEt (670 µL, 3.7 mmol), DMAP (150 mg, 1.3 mmol) and 4-(4-trifluoromethoxyphenyl)-1H-1,2,3-triazole(7, 33) (290 mg, 1.3 mmol) (**25**) were added to the solution. The mixture was stirred for 1.5 h at 50 °C and poured into saturated aqueous NH_4Cl solution. The mixture was extracted with ethyl acetate. The organic layer was washed with H_2O and brine, dried over Na_2SO_4 and concentrated under reduced pressure. The residue was purified by flush column chromatography (ethyl acetate:hexane=1:8 to 1:3) to afford 1,4 triazole urea (**5**, **DO34**) (230 mg, 34%) as top TLC spot. ^{1}H NMR ($CDCl_3$, 600 MHz) δ 7.87−7.79 (m, 2H), 7.57 (s, 1H), 7.32−7.17 (m, 5H), 7.01 (s, 1H), 4.94−4.05 (m, 4H), 3.58−3.49 (m, 1H), 3.23−2.80 (m, 4H), 1.50 (s, 9H). ^{13}C NMR ($CDCl_3$, 150 MHz) 154.89, 149.45, 145.37, 137.10, 129.39, 128.87, 128.34, 127.35, 126.92, 121.57, 120.57 (q, *J* = 256.0 Hz, OCF_3), 80.81, 57.38, 46.73, 43.63, 42.53, 40.60, 36.08, 28.48, 14.28. HRMS calculated for $C_{26}H_{28}F_3N_5O_4$ $[M+H]^+$ 532.2166, found 532.2167.

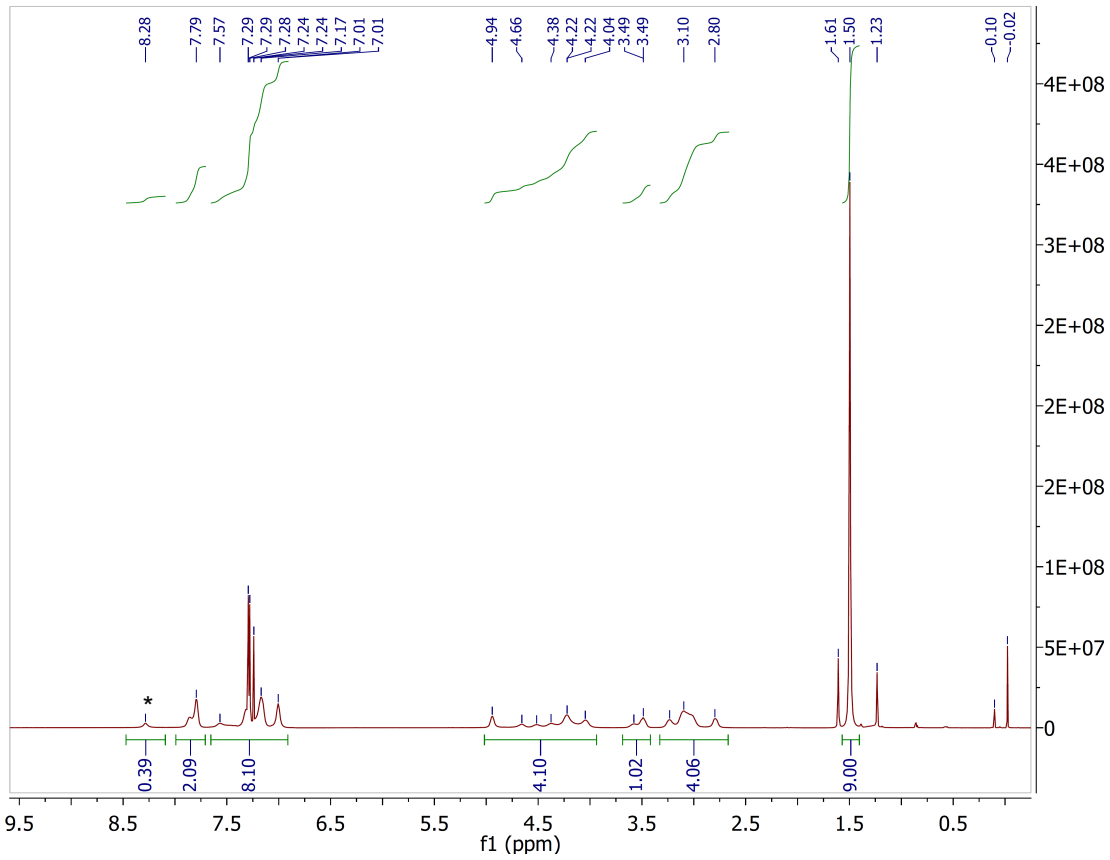
8.28
7.79
7.57
7.29
7.29
7.28
7.24
7.24
7.17
7.01
7.01
4.94
4.66
4.38
4.22
4.22
4.04
3.49
3.49
3.10
2.80
1.61
1.50
1.23
0.10
-0.02
4E+08
4E+08
3E+08
2E+08
2E+08
2E+08
1E+08
5E+07
0
*
0.39
2.09
8.10
4.10
1.02
4.06
9.00
9.5
8.5
7.5
6.5
5.5
4.5
3.5
2.5
1.5
0.5
f1 (ppm)

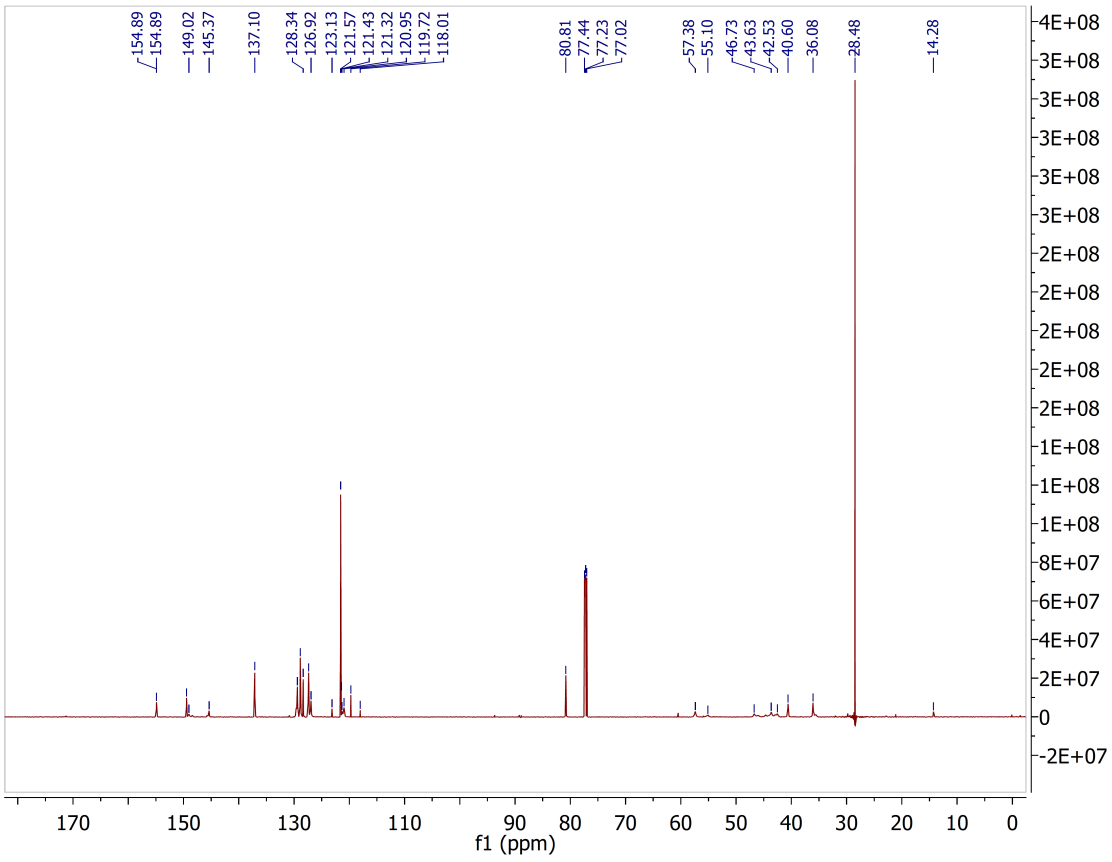
154.89
154.89
149.02
145.37
137.10
128.34
126.92
123.13
121.57
121.43
121.32
120.95
119.72
118.01
80.81
77.44
77.23
77.02
57.38
55.10
46.73
43.63
42.53
40.60
36.08
28.48
14.28
4E+08
3E+08
3E+08
3E+08
3E+08
3E+08
2E+08
2E+08
2E+08
2E+08
2E+08
2E+08
1E+08
1E+08
1E+08
8E+07
6E+07
4E+07
2E+07
0
-2E+07
170
150
130
110
90
80
70
60
50
40
30
20
10
0
f1 (ppm)

Synthesis of (4-{[(2-methyl-2-propanyl)oxy]carbonyl}-2-phenylpyperazinyl){4-[(4-trifluoromethoxy)phenyl]-1H-1,2,3-triazol-1-yl}metanone (7, DO53)

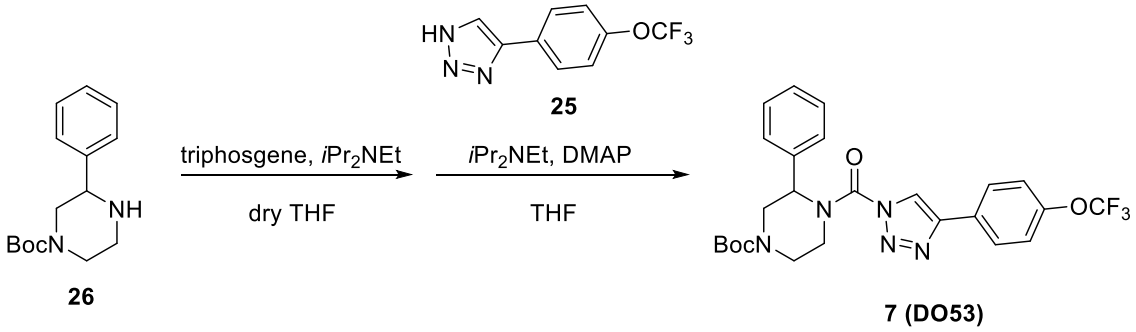

A solution of 1-Boc-3-phenylpiperazine (350 mg, 1.3 mmol) (**25**) in dry THF (9.5 mL) was treated with *i*Pr_2NEt (720 µL, 4.0 mmol) and triphosgene (200 mg, 0.67 mmol), and the reaction mixture was stirred for 30 min at 4 °C. The mixture was poured into H_2O and extracted with ethyl acetate. The organic layer was washed with H_2O and brine, dried over Na_2SO_4 and concentrated under reduced pressure. The residue was dissolved in THF (20 mL), and *i*Pr_2NEt (720 µL, 4.0 mmol), DMAP (160 mg, 1.3 mmol) and 4-(4-trifluoromethoxyphenyl)-1H-1,2,3-triazole (7, 33) (300 mg, 1.3 mmol) (**25**) were added to the solution. The mixture was stirred for 1.5 h at 50 °C and poured into saturated aqueous NH_4Cl solution. The mixture was extracted with ethyl acetate. The organic layer was washed with H_2O and brine, dried over Na_2SO_4 and concentrated under reduced pressure. The residue was purified by flush column chromatography (ethyl acetate:hexane=1:3) to afford 1,4 triazole urea (**7**, **DO53**) (240 mg, 35%) as top TLC spot. ^{1}H NMR ($CDCl_3$, 600 MHz) δ 8.40 (s, 1H), 7.88 (d, 2H, *J* = 8.6 Hz), 7.41−7.24 (m, 7H), 5.84 (s, 1H), 4.68 (s, 1H), 4.41 (s, 1H), 4.13 (s, 0.5H), 3.94 (s, 0.5H), 3.52−3.17 (m, 3H), 1.45 (s, 9H). ^{13}C NMR ($CDCl_3$, 150 MHz) 154.74, 154.37, 149.69, 149.05, 146.01, 136.78, 129.14, 128.29, 128.20, 127.63, 127.13, 121.50, 120.65 (q, *J* = 256.2 Hz, OCF_3), 80.97, 58.68, 45.96,

44.33, 43.09, 28.56, 18.65. HRMS calculated for $C_{25}H_{26}F_3N_5O_4$ $[M+H]^+$ 518.2010, found 518.2009.

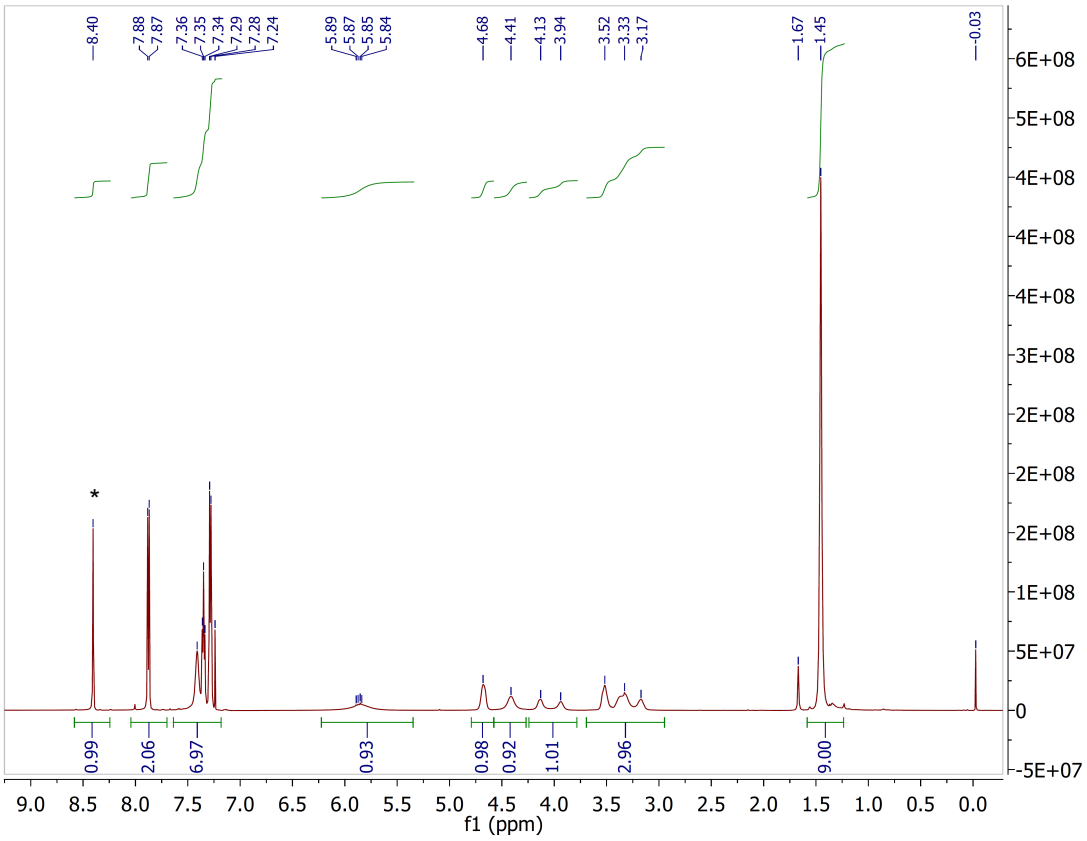

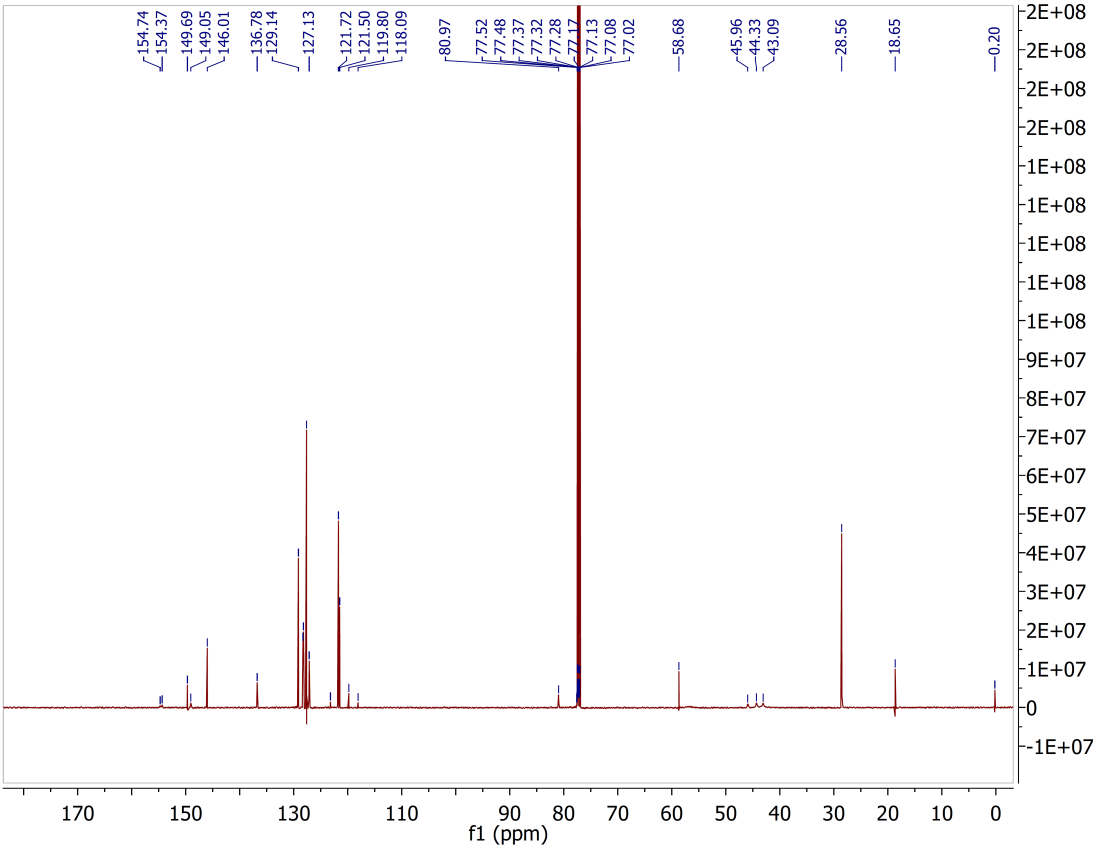
154.74
154.37
149.69
149.05
146.01
136.78
129.14
127.13
121.72
121.50
119.80
118.09
80.97
77.52
77.48
77.37
77.32
77.28
77.17
77.13
77.08
77.02
58.68
45.96
44.33
43.09
28.56
18.65
0.20
2E+08
2E+08
2E+08
2E+08
1E+08
1E+08
1E+08
1E+08
1E+08
9E+07
8E+07
7E+07
6E+07
5E+07
4E+07
3E+07
2E+07
1E+07
0
-1E+07
170
150
130
110
90
80
70
60
50
40
30
20
10
0
f1 (ppm)

Supporting References

1. Liu Y, Patricelli MP, & Cravatt BF (1999) Activity-based protein profiling: the serine hydrolases. *Proc Natl Acad Sci U S A* 96(26):14694-14699.
2. Baggelaar MP*, et al.* (2013) Development of an activity-based probe and in silico design reveal highly selective inhibitors for diacylglycerol lipase-alpha in brain. *Angewandte Chemie* 52(46):12081-12085.
3. Adibekian A*, et al.* (2011) Click-generated triazole ureas as ultrapotent in vivo-active serine hydrolase inhibitors. *Nature chemical biology* 7(7):469-478.
4. Baggelaar MP*, et al.* (2015) Highly Selective, Reversible Inhibitor Identified by Comparative Chemoproteomics Modulates Diacylglycerol Lipase Activity in Neurons. *J Am Chem Soc* 137(27):8851-8857.
5. Kidd D, Liu Y, & Cravatt BF (2001) Profiling serine hydrolase activities in complex proteomes. *Biochemistry* 40(13):4005-4015.
6. Patricelli MP, Giang DK, Stamp LM, & Burbaum JJ (2001) Direct visualization of serine hydrolase activities in complex proteomes using fluorescent active site-directed probes. *Proteomics* 1(9):1067-1071.
7. Hsu K-LL*, et al.* (2012) DAGLβ inhibition perturbs a lipid network involved in macrophage inflammatory responses. *Nature chemical biology* 8(12):999-1007.
8. Janssen FJ*, et al.* (2014) Discovery of glycine sulfonamides as dual inhibitors of sn-1-diacylglycerol lipase α and α/β-hydrolase domain 6. *Journal of medicinal chemistry* 57(15):6610-6622.
9. van der Wel T*, et al.* (2015) A natural substrate-based fluorescence assay for inhibitor screening on diacylglycerol lipase α. *Journal of lipid research* 56(4):927-935.
10. Zweemer AJ*, et al.* (2013) Multiple binding sites for small-molecule antagonists at the CC chemokine receptor 2. *Molecular pharmacology* 84(4):551-561.
11. Bachovchin DA*, et al.* (2010) Superfamily-wide portrait of serine hydrolase inhibition achieved by library-versus-library screening. *Proceedings of the National Academy of Sciences of the United States of America* 107(49):20941-20946.
12. Alexander JP & Cravatt BF (2005) Mechanism of carbamate inactivation of FAAH: implications for the design of covalent inhibitors and in vivo functional probes for enzymes. *Chemistry & biology* 12(11):1179-1187.
13. Nomura DK*, et al.* (2011) Endocannabinoid hydrolysis generates brain prostaglandins that promote neuroinflammation. *Science (New York, N.Y.)* 334(6057):809-813.
14. Lee HC, Simon GM, & Cravatt BF (2015) ABHD4 regulates multiple classes of N-acyl phospholipids in the mammalian central nervous system. *Biochemistry* 54(15):2539-2549.
15. Inloes JM*, et al.* (2014) The hereditary spastic paraplegia-related enzyme DDHD2 is a principal brain triglyceride lipase. *Proceedings of the National Academy of Sciences of the United States of America* 111(41):14924-14929.
16. Kamat SS*, et al.* (2015) Immunomodulatory lysophosphatidylserines are regulated by ABHD16A and ABHD12 interplay. *Nature chemical biology* 11(2):164-171.
17. Martin BR, Wang C, Adibekian A, Tully SE, & Cravatt BF (2012) Global profiling of dynamic protein palmitoylation. *Nature methods* 9(1):84-89.
18. Hulce JJ, Cognetta AB, Niphakis MJ, Tully SE, & Cravatt BF (2013) Proteome-wide mapping of cholesterol-interacting proteins in mammalian cells. *Nature methods* 10(3):259-264.
19. Washburn MP, Wolters D, & Yates JR (2001) Large-scale analysis of the yeast proteome by multidimensional protein identification technology. *Nature biotechnology* 19(3):242-247.
20. Weerapana E*, et al.* (2010) Quantitative reactivity profiling predicts functional cysteines in proteomes. *Nature* 468(7325):790-795.
21. Pan B*, et al.* (2009) Blockade of 2-arachidonoylglycerol hydrolysis by selective monoacylglycerol

lipase inhibitor 4-nitrophenyl 4-(dibenzo[d][1,3]dioxol-5-yl(hydroxy)methyl)piperidine-1-carboxylate (JZL184) Enhances retrograde endocannabinoid signaling. *The Journal of pharmacology and experimental therapeutics* 331(2):591-597.

22. Zhong P*, et al.* (2011) Genetic deletion of monoacylglycerol lipase alters endocannabinoid-mediated retrograde synaptic depression in the cerebellum. *The Journal of physiology* 589(Pt 20):4847-4855.
23. Kreitzer AC & Regehr WG (2001) Retrograde inhibition of presynaptic calcium influx by endogenous cannabinoids at excitatory synapses onto Purkinje cells. *Neuron* 29(3):717-727.
24. Conti B*, et al.* (2006) Transgenic mice with a reduced core body temperature have an increased life span. *Science* 314(5800):825-828.
25. Zorrilla EP*, et al.* (2007) Interleukin-18 controls energy homeostasis by suppressing appetite and feed efficiency. *Proc Natl Acad Sci U S A* 104(26):11097-11102.
26. Sanchez-Alavez M*, et al.* (2007) Night eating and obesity in the EP3R-deficient mouse. *Proc Natl Acad Sci U S A* 104(8):3009-3014.
27. Sanchez-Alavez M*, et al.* (2010) Insulin causes hyperthermia by direct inhibition of warm-sensitive neurons. *Diabetes* 59(1):43-50.
28. Velmourougane G*, et al.* (2011) Synthesis of new (-)-bestatin-based inhibitor libraries reveals a novel binding mode in the S1 pocket of the essential malaria M1 metalloaminopeptidase. *Journal of medicinal chemistry* 54(6):1655-1666.
29. Blacker AJ*, et al.* (2011) Convenient Method for Synthesis ofN-Protected α-Amino Epoxides: Key Intermediates for HIV Protease Inhibitors. *Organic Process Research & Development* 15(2):331-338.
30. van den Nieuwendijk AMCH, Ghisaidoobe ABT, Overkleeft HS, Brussee J, & van der Gen A (2004) Conversion of chiral unsaturated cyanohydrins into chiral carba- and heterocycles via ring-closing metathesis. *Tetrahedron* 60(46):10385-10396.
31. Adibekian A*, et al.* (2010) Optimization and characterization of a triazole urea inhibitor for alpha/beta hydrolase domain-containing protein 11 (ABHD11): anti-probe for LYPLA1/LYPLA2 dual inhibitor ML211. *Probe Reports from the NIH Molecular Libraries Program*, Bethesda (MD)).
32. Verdoes M*, et al.* (2008) Azido-BODIPY acid reveals quantitative Staudinger-Bertozzi ligation in two-step activity-based proteasome profiling. *Chembiochem* 9(11):1735-1738.
33. Hsu K-LL*, et al.* (2013) Development and optimization of piperidyl-1,2,3-triazole ureas as selective chemical probes of endocannabinoid biosynthesis. *Journal of medicinal chemistry* 56(21):8257-8269.